Dynamic line rating implementation as an approach to handle wind power integration

A feasibility analysis in a sub-transmission system owned by Fortum Distribution AB

SAIFAL TALPUR

KTH Electrical Engineering

Degree project in
Electromagnetic Engineering
Second Level, 30.0 HEC
Stockholm, Sweden 2013

XR-EE-ETK 2013:002

Dynamic line rating implementation as an approach to handle wind power integration

A feasibility analysis in a sub-transmission system owned by Fortum Distribution AB

Saifal Talpur

Master Thesis

EI255X

Supervisors

Christer Flood

Carl Johan Wallnerström

Examiner

Patrik Hilber

Department of Electromagnetic Engineering

School of Electrical Engineering

The Royal Institute of Technology (KTH)

Stockholm, 2013

ACKNOWLEDGMENTS

This diploma work is done in collaboration between KTH and Fortum Distribution AB.

First of all, I would like to thank the Almighty Allah who enabled me to complete this degree project and helped me in completing the coursework of my degree.

Thereafter, I am thankful to Christer Flood who not only trusted on my abilities and provided me the opportunity to carry out this project at Fortum Distribution AB (a leading power company) but also guided me a lot in the project. I am also thankful to my supervisor at KTH, Carl Johan for his thorough guidance regarding the report writing.

I would like to thank Mr. Olle Hansson who helped me in getting a seat at the office of Fortum Distribution AB in Stockholm. I would also be very grateful of Patrik Hilber, my examiner at KTH, for proofreading of my report.

I would pay special thanks to my mom and dad for having a trust on me to complete my degree as well as for their moral and financial support. Many thanks go to my brother and sister, Mudasir and Zoya as well for their encouragement throughout my stay in Stockholm.

Last but not least, after getting a seat at the Stockholm office of Fortum Distribution AB, I enjoyed a professional working environment in a leading power industry that could be beneficial for my career.

ABSTRACT

Based on conventional static line rating method, the actual current carrying capability of overhead conductors cannot be judged. Due to continuous increment in electricity demand and the difficulties associated with new line constructions, the overhead lines are therefore required to be rated based on a method that should establish their real-time capability in terms of electricity transmission. The method used to determine the real-time ampacity of overhead conductors not only can enhance their transmission capacity but can also help in allowing excessive renewable generation in the electricity network. In this diploma work, the issues related to analyzing an impact of wind power on periodical loading of overhead line as well as finding its static and dynamic ampacities with line current are investigated in detail.

Initially, in this project, the investigation related to finding a suitable location for the construction of a 60 MW wind farm is taken on board. Thereafter, the wind park is integrated with a regional grid, owned by Fortum Distribution AB. In addition to that, the electricity generated from the wind park is also calculated in this project. Later on, the work is devoted to finding the static and dynamic line ratings for 'VL3'overhead conductor by using IEEE-738-2006 standard.

Furthermore, the project also deals with finding the line current and making its comparison with maximum capacity of overhead conductor (VL3) for loading it in such a way that no any violation of safe ground clearance requirements is observed at all. Besides, the line current, knowing the conductor temperature when it transmits the required electricity in the presence of wind power generation is also an important factor to be taken into consideration. Therefore, based on real-time ambient conditions with actual line loading and with the help of IEEE-738-2006 standard, the conductor temperature is also calculated in this project.

At the end, an economic analysis is performed to evaluate the financial advantages related to applying the dynamic line ratings approach in place of traditional static line ratings technique across an overhead conductor (VL3) and to know how much beneficial it is to temporarily postpone the rebuilding and/or construction of a new transmission line. Furthermore, an economic analysis related to wind power system is taken into consideration as well to get familiar with the costs related to building and connecting a 60 MW wind farm with the regional grid.

Keywords: Regional grid, overhead conductor, wind power, real-time weather, dynamic line rating, static line rating, line current, conductor temperature, ampacity upgrading, economics.

LIST OF FIGURES

LIST OF TABLES

CONTENTS

List of Acronyms

SLR: Static Line Rating

DLR: Dynamic Line Rating

PSS/E©: Power System Simulator for Engineering

SMHI: Swedish Metrological & Hydrological Institute

IEEE: Institute of Electrical & Electronics Engineers

DSO: Distribution System Operator

OH-Line: Overhead Line

ACSR: Aluminum Conductor Steel Reinforced

RMS: Root Mean Square

AC: Alternating Current

DC: Direct Current

ATC: Available Transmission Capacity

PV: Present Value

NPV: Net Present Value

SEK: Swedish Krona

EUR: Euro (€)

USD: US Dollar ($)

Chapter 1

Introduction

This chapter covers an introduction about the work carried out in this project and also includes purpose and outline of the chapters.

1.1 Background

Due to limited capacity of fossil fuels, the world is focusing on the usage of renewable power generation in terms of electricity production and fulfilling its growing demand. Hence, it will not be wrong to say that renewable power generation will be a significant source of energy in the near future. Furthermore, amongst many notable green energy sources, the wind energy is also a pollution free energy source with a long-term availability (almost the whole year) making it a suitable alternate to other energy sources, however its only disadvantage is its day to day unreliability [1].

Now, in this project, based on a real case study, 60 MW of wind power generation was added in a 130 kV sub-transmission system and its role was investigated in terms of line loading. Besides this task, the calculation of static and dynamic line ratings (DLR) of an overhead conductor and their comparison with the line current were taken on board.

Furthermore, static line rating (SLR) is actually based on worst weather conditions and does not consider any real-time line rating approach [2]. Contrary to that, the DLR technique is based on real-time data and helps in finding the actual capacity of overhead conductors in delivering the electric power [2]. Historically, the transmission lines were operated at their static or fixed ratings and based on these ratings, the transfer of electric power was limited to a large extent, making it difficult to know the actual maximum capacity of overhead lines [2].

With the help of DLR approach, the overhead transmission lines can carry the maximum current that may help in fulfilling the growing demand of electricity without investing huge money on rebuilding the existing transmission lines and/or constructing new transmission lines to carry the required amount of maximum electric power [2]. Hence, based on this approach, massive direct or indirect economical savings can be obtained with a considerable reliability [2]. Moreover, it may still be significant, if the planning of rebuilding and /or construction of new transmission lines is delayed on temporary basis [3].

Now, based on the nature of dynamic line rating, the real-time weather data related to ambient temperature, wind speed and its direction was first gathered in this project before calculating the DLR. This data was based on Karlstad municipality of Sweden and was obtained from the Swedish Metrological and Hydrological Institute (SMHI) [4].

1.2 Purpose

An important goal of this project is to evaluate the technical and economical aspects of dynamic line rating across an overhead conductor (VL3) in a meshed 130 kV sub-transmission electricity network.

Now, based on the case study, following specific objectives were formulated in this project:

- Evaluation of wind speed and its direction (relative to the axis of line conductor) on the wind power production
- Development of a system model of the wind power connection with the 130 kV grid
- Assessment of power flow study after wind power connection in the sub-transmission network
- Investigation of the profits regarding DLR implementation in place of costly conventional ampacity upgrading techniques

1.3 Outline

This diploma work is arranged in six chapters; a brief overview of each chapter is mentioned as follows:

Chapter 2 (Dynamic Rating & Wind Power Generation) describes the theoretical and mathematical summary of ambient weather conditions, wind power generation, the load flow study and the dynamic line rating. Moreover, this chapter is accompanied with figures, charts, mathematical equations and some technical discussion.

Chapter 3 (Wind Power Analysis) gives a detailed analysis of how ambient conditions affect the wind power generation and takes into account a comprehensive discussion related to finding a suitable location of the wind farm, analyzing the wind roses, examining the wind speed and its direction and evaluating the output electrical power from the specific installed wind turbines.

Chapter 4 (Dynamic Line Rating) focuses on static and dynamic line ratings of an overhead conductor. Moreover, in this chapter, the investigation related to line current in the presence of wind power generation and checking its effect on conductor temperature is taken into account as well. Comparison amongst different line ampacities is another important factor discussed in this chapter.

Chapter 5 (Economic Analysis) is devoted to an economic analysis. The questions related to how much profit a utility may earn in terms of enhancing the power transfer capability of an overhead transmission line and how much savings it may receive after having postponed the upgrading and/or construction of a new line are some issues discussed in detail with the help of reliable mathematical calculations.

Chapter 6 (Conclusion, Discussion and Future Work) is dedicated to conclusion, discussion and the future work. Which milestones are obtained successfully in this project and which need to be obtained are discussed in detail.

Chapter 2

Dynamic Rating and Wind Power Generation

This chapter starts with a brief introduction of dynamic rating followed by theoretical and mathematical summary of weather conditions, wind power generation, and the load flow study of the power lines.

2.1 Dynamic Rating

The dynamic rating is considered a real time or near real time rating approach that determines the conductor ampacity leading to cause the maximum allowable conductor temperature under real-time weather conditions [5]. Contrary to that, the static rating is assumed a fixed rating and is calculated based on some assumptions related to fixed weather parameters [5]. The disadvantage of static rating as compared to the dynamic is that when any power system component is operated under fixed rating system, then its capacity of transmitting the maximum electric power is not fully utilized [2]. Due to its significant technical and economic advantages, the power utilities are considering to update their systems based on real-time dynamic rating system and these advantages have now made the power system operators aware that of how much rating the components can be operated without violating their design limits and utilizing all the transmission resources to the fullest [2].

The dynamic rating moreover, reflects the accurate rating of the power system components. By using the dynamic rating, the real time information about component's ability to deliver the electrical power can be easily obtained. The transmission line conductors are required to transmit the electric power until their allowable thermal rating is not crossed [2]. Now, for describing the dynamic line rating of any overhead conductor, following parameters should be known in advance [2]:

- Ambient temperature
- Wind speed
- Direction of the wind speed with respect to the conductor alignment
- Solar radiation
- The assumed maximum allowable conductor temperature
- Line loading
- Conductor characteristics

The decision of using dynamic line rating instead of static line rating is related to the available transmission capacity (ATC) of overhead conductors [2]. The reason is that the available transmission line capacity cannot be approximated correctly by using static rating of the transmission lines [2]. However, on the other hand, dynamic line rating may always help in determining actual information regarding the conductor's transmission capacity [2].

2.2 Wind Power Generation

The renewable energy sources exist in many forms, the notable amongst them are the hydro power, solar power, wind power, tidal power and the geothermal energy. The availability of renewable energy sources varies with respect to type of land [6]. Due to non-uniformity in the existence of renewable energy, a part of the world that dominates for example in solar power may or may not be observed with abundant wind energy. However, the availability of renewable energy is different than its implementation in terms of electricity generation. For example, there are still some parts of the world (particularly the developing nations) that are found with excess renewable energy but are unable to make their implementation, mainly due to financial issues like high interest rates and short-term loans assigned for renewable energy projects [7].

As compared to other renewable energy sources, the overall trend of getting electricity from the wind power is getting increased in the world. According to the latest figures about the wind power generation, an overwhelming importance of this green energy is observed throughout the world. It is estimated that there are around 200,000 wind turbines installed all over the world with a total installed capacity of around 283 GW at the end of 2012 [8]. Only in Europe, the total nameplate installed capacity of wind turbines was observed around 100 GW in the year of 2012 [9], whereas, in the United States, it reached around 50 GW, during the same year [10].

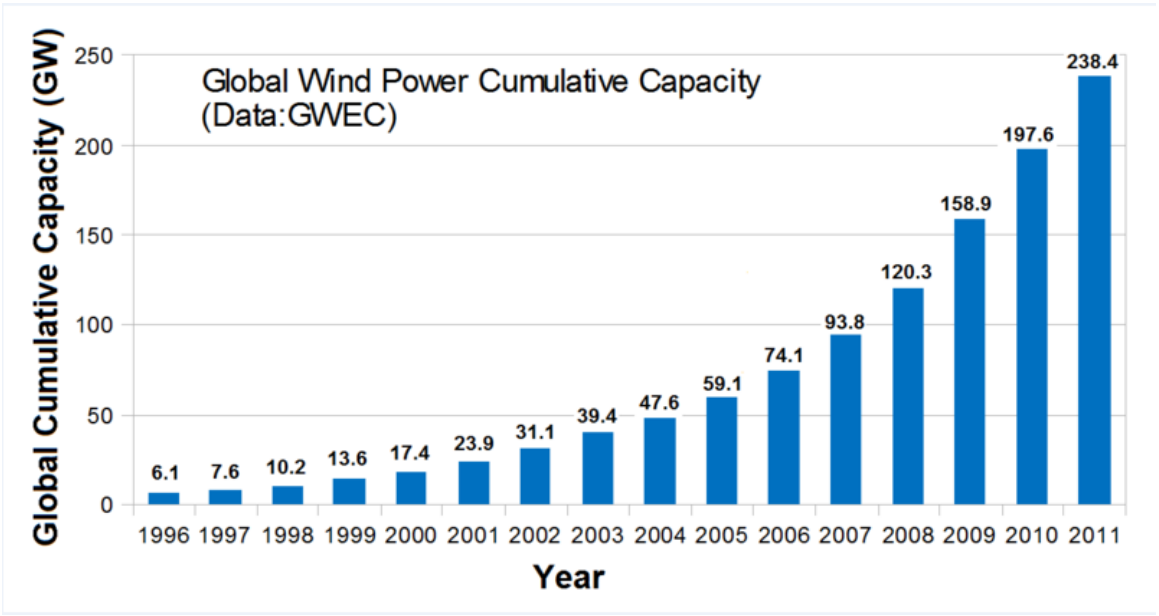

Figure 2.1: A yearly overview of global wind power installed capacity [11]

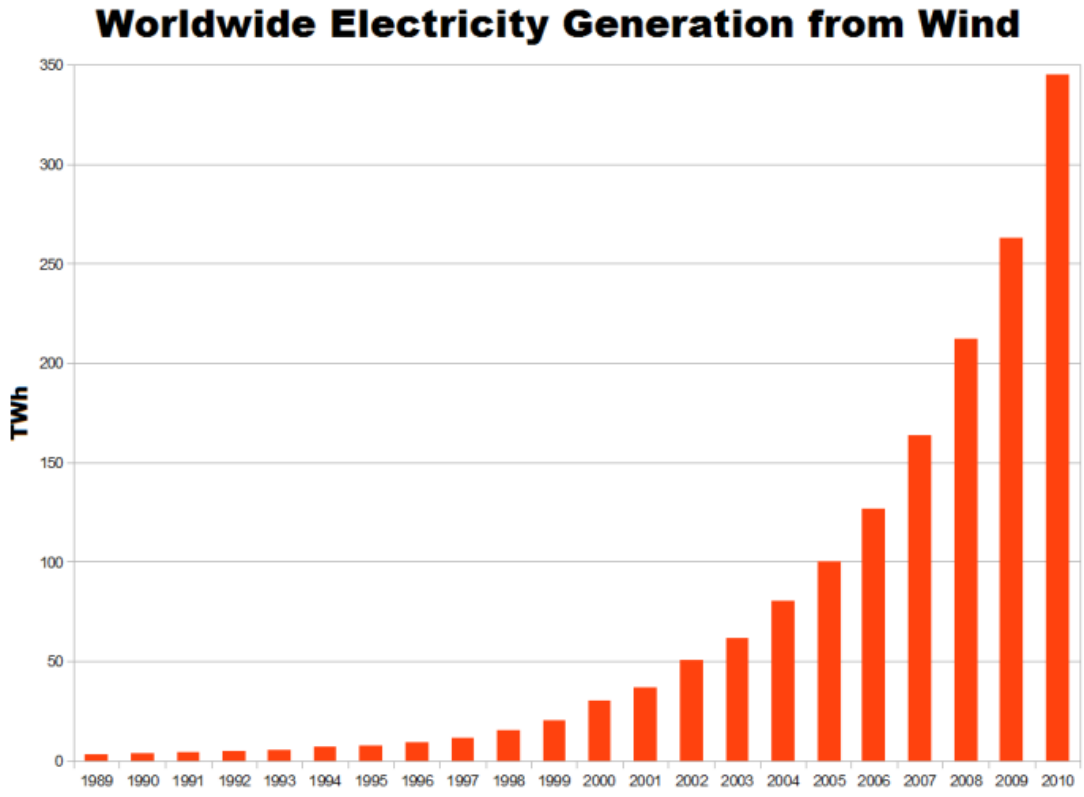

Figure 2.2: Global electricity generation from the wind power [11]

Wind is actually produced due to changes in atmospheric temperature and pressure. It can be termed as a flow of air and helps in producing the kinetic energy, which ultimately leads towards moving the wind turbine blades.

Mathematically, the kinetic energy k can be represented with the help of equation 2.1 [12], i.e.

$$k = \frac{1}{2} * m * {v_1}^2 \quad (j) \tag{2.1}$$

The kinetic energy further helps in producing the power P that wind energy contains and is expressed in equation 2.2 [12], i.e.

$$P = \frac{\rho}{2} A {v_1}^3 \quad (W) \tag{2.2}$$

Where, ρ is the specific air mass that depends upon the air pressure and moisture and A is the circular swept area. For many practical applications, it is assumed that $\rho \approx 1.25\ {}^{kg}/_{m^3}$ [12]. Now, for obtaining the mechanical power P (given in equation 2.3) [12], equation 2.2 is multiplied with the power co-efficient c_p , i.e.

$$P = c_p \frac{\rho}{2} A {v_1}^3 \quad (W) \tag{2.3}$$

In practice, the wind speed (v_1) that strikes at the blades differs from the wind speed that is observed behind the blades v_3. It is due to the fact that when the air strikes at the wind turbine blades, it is observed quite smooth while after hitting at the blades it becomes rather non-homogenous [12]. Now, from equation 2.3, it is obvious that with small increase in wind speed, the mechanical power gets increased to a large extent. Moreover, the maximum mechanical power is obtained when $\frac{v_1}{v_3} = \frac{1}{3}$ [12]; at this ratio, the power co-efficient becomes equal to: $c_p = \frac{16}{27} \approx 0.59$ [12].

An important factor in terms of designing the wind turbine blades is called the tip speed ratio λ. In the modern two and three bladed wind turbines, the maximum tip speed ratio (λ) is kept 10 and 7 respectively [12]. Furthermore, the wind turbines installed at mountainous surfaces face low friction as compared to those installed at ground due to buildings, trees and other objects [12]. Similarly, the wind turbines installed at the offshore enjoy the maximum potential of wind energy but the only drawback of installing the wind turbines at offshore is their complex and expensive maintenance.

Now, assuming that the wind speed 'v_1' at a certain height 'z_1' is known, similarly, the height 'z_2' is also known then based on these known parameters, the wind speed 'v_2' at height 'z_2' can be calculated with the help of mathematical expression 2.4 [13], i.e.

$$v_2(z_2) = v_1 \frac{\ln\left(z_2/z_0\right)}{\ln\left(z_1/z_0\right)} \tag{2.4}$$

z_o here represents the roughness length and it mainly depends upon the land of the country. It is actually measured on the basis of surface roughness that on the other hand affects the flow of air [14]. The roughness length is classified into different categories depending upon the nature of surface. For example, in case of open flat areas, it is assumed to be 0.03 m [14], whereas for forests, it varies between 0.5 m to 1 m [14]; similarly, in case of croplands, it ranges in between of 0.1 m to 0.25 m [14].

2.3 Load Flow Study

The load flow study is related to analyzing the static power flow through overhead lines. In this section, the load flow study of a simple power system is mentioned in detail. Now, considering a simple power system as shown in figure 2.3 with two generation sources; a wind farm and a conventional power plant with one passive load, the load flow study then based on this power system is described in this section.

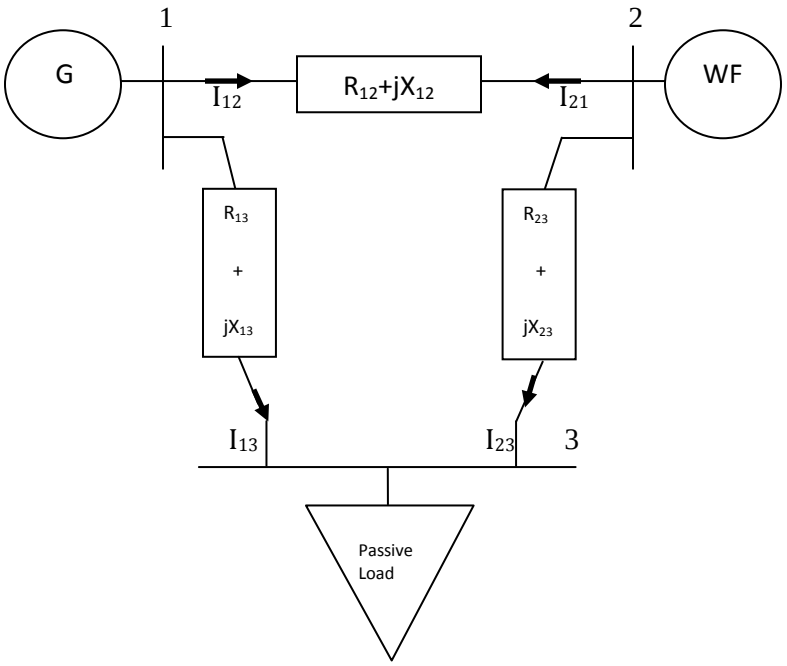

Figure 2.3: A simple Power System

For analyzing a simple power system in figure 2.3, the power flow equations are required to be developed based on the pi-equivalent model as shown in figure 2.4.

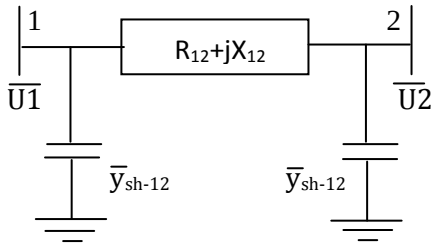

Figure 2.4: π-equivalent model of a line

Now, based on a pi-equivalent model (figure 2.4) of a transmission line connected in between of ports 1 and 2, the power flow between these nodes can be then calculated with the help of following equations, i.e.

Similarly, based on figure 2.4, the two port equations (2.5 and 2.6) [15] are given as:

$$\overline{U_1} = \overline{U_2} + (\overline{I_2} + \overline{U_2} \cdot \overline{y_{sh-12}}) * \overline{Z_{12}} \tag{2.5}$$

$$\overline{I_1} = \overline{U_1} \cdot \overline{y_{sh-12}} + \overline{I_2} + (\overline{U_2} \cdot \overline{y_{sh-12}}) \tag{2.6}$$

Now, re-arranging the equations 2.5 and 2.6 yields:

$$\overline{U_1} = (1 + \overline{Z_{12}} \cdot \overline{y_{sh-12}}) * \overline{U_2} + \overline{Z_{12}} \cdot \overline{I_2} \tag{2.7}$$

$$\overline{I_1} = \overline{y_{sh-12}} * (2 + \overline{Z_{12}} \cdot \overline{y_{sh-12}}) * \overline{U_2} + (1 + \overline{Z_{12}} \cdot \overline{y_{sh-12}}) \cdot \overline{I_2} \tag{2.8}$$

In terms of matrix notation, these two port equations can be represented as:

$$\begin{bmatrix} \overline{U_1} \\ \overline{I_1} \end{bmatrix} = \begin{bmatrix} 1 + \overline{Z_{12}} \cdot \overline{y_{sh-12}} & \overline{Z_{12}} \\ \overline{y_{sh-12}} * (2 + \overline{Z_{12}} \cdot \overline{y_{sh-12}}) & 1 + \overline{Z_{12}} \cdot \overline{y_{sh-12}} \end{bmatrix} \tag{2.9}$$

Now, in case of a short transmission line model, $\overline{y_{sh-12}} = 0$ and based on this assumption related to a short-line model, the two port equations [15] will be then:

$$\begin{bmatrix} \overline{U_1} \\ \overline{I_1} \end{bmatrix} = \begin{bmatrix} 1 & \overline{Z_{12}} \\ 0 & 1 \end{bmatrix} * \begin{bmatrix} \overline{U_2} \\ \overline{I_2} \end{bmatrix} \tag{2.10}$$

or,

$$\overline{U_1} = \overline{U_2} + \overline{Z_{12}} \cdot \overline{I_2} \quad (2.11)$$

$$\overline{I_1} = \overline{I_2} \quad (2.12)$$

Similarly, the flow of current from node 1 towards the node 2 is actually based on the voltage difference between these nodes [15], and is shown in equation 2.13 [15], i.e.

$$\overline{I_{12}} = (\overline{U_1} - \overline{U_2}) * (G_{12} + jB_{12}) \quad (2.13)$$

Moreover, the current flowing from node 2 towards node 1 is identical to the current flowing from node 1 towards node 2 and can be represented as:

$$\overline{I_1} = -\overline{I_2} \quad (2.14)$$

where,

1 ⟶ represents the bus from which the current is coming

2 ⟶ represents the bus towards which the current is going

Similarly,

G represents the conductance and *B* represents the susceptance.

Now, the active power losses across a short transmission line based on flow of current can be easily calculated with the help of equations 2.15[16] and 2.16[16], i.e.

$$S_{12} = \overline{U_1} * \overline{I_{12}}^{*} \quad (VA) \quad (2.15)$$

Similarly,

$$S_{21} = \overline{U_2} * \overline{I_{21}}^{*} \quad (VA) \quad (2.16)$$

Moreover, the total line losses $S_{L\,12}$ across a transmission line between two voltage sources $\overline{U_1}$ and $\overline{U_2}$ will be:

$$S_{L\,12} = S_{12} + S_{21} \ (VA) \quad (2.17)$$

In addition to that, the total line losses consist of both active and reactive power losses. The active power losses P_{L12} are calculated with the help of equation 2.18 [16], i.e.

$$P_{L12} = {I_{RMS,12}}^2 * R_{12} \ (W) \tag{2.18}$$

where,

R_{12} is the effective resistance and $I_{RMS,12}$ is the RMS current between the transmission lines 1 and 2.

Now, when a transmission line does not contain any reactive component then power losses are calculated on the basis of resistance only as shown in equation 2.18 [16]. However, that may only happen when a line is either short (where line contains only inductive component) in length or it is operated by DC Voltage (no inductive and capacitive components due to zero frequency) [16]. But for medium and/or long transmission lines, the capacitive component cannot be neglected [16].

Now, considering a short transmission line between two voltage sources, $\overline{U_1}$ and $\overline{U_2}$ with the ohmic loss P_{L12} as shown in equation 2.19 [16] is given as:

$$P_{L12} = {I_{RMS,12}}^2 * R_{e,12} \ (\overline{Z_{12}}) \ \ (W) \tag{2.19}$$

Here,

$R_{e,12}$ represents the real component of $\overline{Z_{12}}$.

$\overline{Z_{12}}$ is the complex impedance of the transmission line that contains the resistive, inductive and capacitive components [16], i.e.

$$\overline{Z_{12}} = (R_{12} + jX_{12}) \quad (\Omega)$$

Moreover, all these resistive R_{12} and reactive X_{12} components are measured in ohms and are taken at per unit length of an overhead conductor, measured in meters.

2.4 Dynamic Line Rating

The dynamic line rating is related to implementation of real-time information to develop accurate ratings for the overhead conductors [2]. This precise information helps in utilizing the full capacity of conductors in terms of transmitting the required electric power. With the help of DLR technique, thermal rating of a conductor based on its real-time temperature (or current) can be calculated dynamically [17]. Furthermore, the implementation of DLR approach can be helpful in terms of adjusting the power supply and hence the load demand in real-time [17].

Here, in this section, equations related to finding the dynamic line rating based on real-time weather data and the line loading is developed for knowing the effect of ambient data on line ratings. Similarly, when an overhead conductor carries the maximum current, it will be able to fulfill the increasing load requirements and certainly will help in postponing/avoiding the construction of new transmission lines [2]. This short or long term postponing of installing the new transmission conductors or the transformers is useful for a utility from economical, political, social and environmental perspectives [2].

Now, with the help of equations 2.20-2.33 (based on IEEE-738-2006 Standard[1]), the dynamic line rating of the overhead conductors (equation 2.34) can be easily calculated. Furthermore, the S.I units and the specifications of the parameters used in these equations are listed in table 2.1, i.e.

Table 2.1: Parameters for the Dynamic Line Rating

PARAMETER (S)	SPECIFICATION (S)	SI Units
R_{T_C}	AC resistance of conductor i at temperature Tc	Ω/m
I_i	Current through conductor i	A
β_i	Solar absorptivity of conductor i	_____
φ	Total solar and sky radiated heat flux rate	W/m^2
θ	Effective angle of incidence of sun rays	degrees

$A_{p,i}$	Projected area of conductor i per unit length	m^2/m
D_i	Diameter of conductor i	mm
T_A	Ambient temperature	°C
T_C	Conductor temperature	°C
T_{high}	Max. Conductor temperature	°C
T_{low}	Min. Conductor temperature	°C
σ	Density of air	kg/m^3
V_w	Speed of wind at conductor i	m/s
α	Thermal conductivity of air at temperature T_{film}	W/(m-°C)
ε	Dynamic viscosity of air	Pa-s
$\in_i$	Emissivity of conductor i	_____
K_{angle}	Wind direction factor	_____
ϕ	Angle between wind and conductor axis	degrees
T_{film}	Film Temperature	°C
h_e	Conductor elevation above sea	m

Moreover, based on different observations, it is clear that the conductor temperature varies with respect to heat input (gain rate) and heat output (loss) sources. The heat input (heat gained by the conductor) observed across the OH-conductor is due to ohmic losses and the solar heat gain (solar radiation or solar flux) [18]. After being heated up, the heat energy gained by the conductor is lost by means of two factors, i.e. convection and radiation [18], known as heat output sources.

According to the law of conservation of energy, there should always be a balance between heat gain and heat loss rates, i.e. the heat balance equation 2.20 [19] must be followed all the times in terms of determining the conductor ampacity rating [19].

$$Heat_{GAIN} = Heat_{LOSS} \tag{2.20}$$

The following heat balance equation [19] represents the balance amongst heat gain and heat loss rates, i.e.

$$P_{loss} + Q_{solar} = Q_{convection} + Q_{radiation} \tag{2.21}$$

The ohmic loss P_{loss} (W) causes heat gain in the conductor and is calculated based on equations 2.22 [19] and 2.23 [19], i.e.

$$P_{loss} = {I_i}^2 * R_{T_C} \tag{2.22}$$

$$R_{T_C} = \left[\frac{R_{T_{high}} - R_{T_{low}}}{T_{high} - T_{low}}\right] * (T_C - T_{low}) + R_{T_{low}} \tag{2.23}$$

Similarly, the solar heat gain can be calculated with the help of equation 2.24 [19]. From this equation, it is observed that this heat gain (Q_{solar}) depends upon five main factors, i.e. on the projected conductor area, conductor's ability of absorbing sun rays, the conductor latitude, the number and timing of the day.

$$Q_{solar} = \beta_i \varphi \sin(\theta) A_{p,i} \tag{2.24}$$

Furthermore, the heat loss rate is classified into two types, i.e. the heat loss due to convection and the heat loss due to radiation [18]. The convection heat loss rate is further classified into two types; the natural convection and the forced convection [19]. The natural convection heat loss rate depends upon the difference in temperature between ambient and conductor [20]. This heat loss rate Q_{NC} (W/m) is dependent upon conductor diameter, the temperature across conductor and the ambient temperature [18]. It can be calculated with the help of equation 2.25 [19], i.e.

$$Q_{NC} = 0.0205 * \sigma^{0.5} * {D_i}^{0.75} * \left(T_{C,i} - T_A\right)^{1.25} \tag{2.25}$$

The forced convection heat loss rate mainly depends upon wind speed and its direction [18]. This heat loss rate is also classified into two categories, depending upon the magnitude of wind speed. At low wind speeds (lower than 4.47 m/sec [19]), the forced convection heat loss rate Q_{FC_low} (W/m) will be calculated based on equation 2.26 [19], i.e.

$$Q_{FC\_low} = \left[1.01 + 0.0372 \left(\frac{D_i * \sigma * V_w}{\varepsilon}\right)^{0.52}\right] * \alpha * K_{angle} * \left(T_{C,i} - T_A\right) \qquad (2.26)$$

Similarly, at high wind speeds (higher than or equal to 4.47 m/sec [19]), the forced convection Q_{FC_high} (W/m) is calculated with the help of equation 2.27 [19].

$$Q_{FC\_high} = \left[0.0119 \left(\frac{D_i * \sigma * V_w}{\varepsilon}\right)^{0.6} * \alpha * K_{angle} * \left(T_{C,i} - T_A\right)\right] \qquad (2.27)$$

Moreover, in case of low wind speeds, the larger amongst natural and forced convection methods should be used [19]. At zero wind speed, the forced convection heat loss rate will be zero but during that state, the natural convection method will work and will help in reducing the conductor temperature [19]. Finding the forced convection heat loss rate, needs the wind direction factor (K_{angle}) to be calculated and is given in equation 2.28 [19], i.e.

$$K_{angle} = 1.194 - \cos(\phi) + 0.194 * \cos(2\phi) + 0.368 \sin(2\phi) \qquad (2.28)$$

Now, considering the thermal conductivity of air (α) at temperature T_{film} as given in equation 2.29 [19].

$$\alpha = 2.424 * 10^{-2} + 7.477 * 10^{-5} * T_{film} - 4.407 * 10^{-9} * T^2{}_{film} \qquad (2.29)$$

The average of ambient and conductor temperatures (T_{film}) is given in equation 2.30 [19], i.e.

$$T_{film} = \frac{T_{c,i} + T_A}{2} \qquad (2.30)$$

Now, the equation 2.31 [19] represents the dynamic viscosity of surrounding air, i.e.

$$\varepsilon = \frac{1.458 * 10^{-6}\left(T_{film} + 273\right)^{1.5}}{T_{film} + 383.4} \qquad (2.31)$$

The air density can be calculated based on equation 2.32 [19], i.e.

$$\sigma = \frac{1.293 - 1.525 * 10^{-4} * h_e + 6.379 * 10^{-9} * {h_e}^2}{1 + 0.00367 * T_{film}} \tag{2.32}$$

The equation 2.33 from IEEE-standard [19] gives the radiated heat loss rate $Q_{radiation}$ (W/m), i.e.

$$Q_{radiation} = 0.0178 * D_i * \in_i * \left[\left(\frac{T_{C,i} + 273}{100}\right)^4 - \left(\frac{T_A + 273}{100}\right)^4\right] \tag{2.33}$$

The radiated heat loss rate same like the forced convection heat loss rate depends upon the difference in temperature between conductor and ambient. The higher this difference the higher will be the radiation heat loss rate. After knowing the values of heat gain and heat loss parameters, the ampacity of conductor i can be calculated with the help of equation 2.34 [19], i.e.

$$I_i = \sqrt{\frac{(Q_{convection} + Q_{radiation}) - Q_{solar}}{R_{T_C}}} \quad (A) \tag{2.34}$$

Now, based on conductor's ampacity as shown in equation 2.34, it is evident that the convection and radiation heat loss rates increase conductor's capacity in terms of enabling it to transfer maximum electricity. Similarly, the conductor's ampacity can be increased when the solar radiation is lower. Moreover, the thermal AC resistance also plays its role in terms of determining the ampacity of the overhead line.

[1]IEEE-738-2006 Standard is used to determine the relationship between current and temperature across the bare overhead conductors [19].

Chapter 3

Wind Power Analysis

Selecting the decisive location of a wind farm and installing the suitable wind turbines to get required amount of electric power with the help of suitable tools are some important issues, discussed in this chapter.

3.1 Installation of wind turbines

Technological advancements in power electronics has increased the scope of wind power system [21]. Because, due to unstable nature of wind speed and its direction, keeping the system voltage and frequency to its constant level requires a frequent usage of power electronic equipments [21]. With the help of power electronic converters, a constant electric power is sent to the active and/or passive loads at almost constant voltage [21].

Now, before installation of the wind turbines, a suitable location of the wind farm must be decided in advance. In order to find a suitable location for construction of a wind farm, it is required to consider many factors, some important ones [12] are:

- A large and open flat area
- Access to the road to carry out flexible installation and maintenance
- Access to the national/regional grid
- Low noise effect in the area
- Abide by air traffic rules
- Taking into account the safety rules in terms of ice fallings
- Away from the protected areas

It is important that besides considering the technical benefits, environmental and social perspectives should be taken on board as well, so that a widely accepted location of the wind farm is chosen. Now, in this project, a wind farm consisting of 20 Enercon E-101 wind turbines is constructed based on a flexible access with the regional grid. Moreover, the planned installed capacity of this wind farm is chosen around 60 MW. The location of this wind farm is planned in an open area at Stöpsjön (in the province of Värmland county, Sweden), having a distance of only 10 km from a 130 kV regional grid (in the municipality of Filipstad, Sweden). Now, after consideration of planned location for the wind farm, it was

required to find an optimal direction of the wind turbines. Moreover, the decision related to finding a suitable direction of the wind turbines was based on the results from wind roses. A wind rose is actually an important tool used in terms of making the decision regarding the dominant direction of wind speeds during a single year. Here, in this project, the data related to wind speed and its direction was obtained from SMHI (Swedish Metrological and Hydrological Institute) for a hub-height of 100 m and then based on this data; a wind rose was plotted with the help of Enviroware© Software and is shown in figure 3.1.

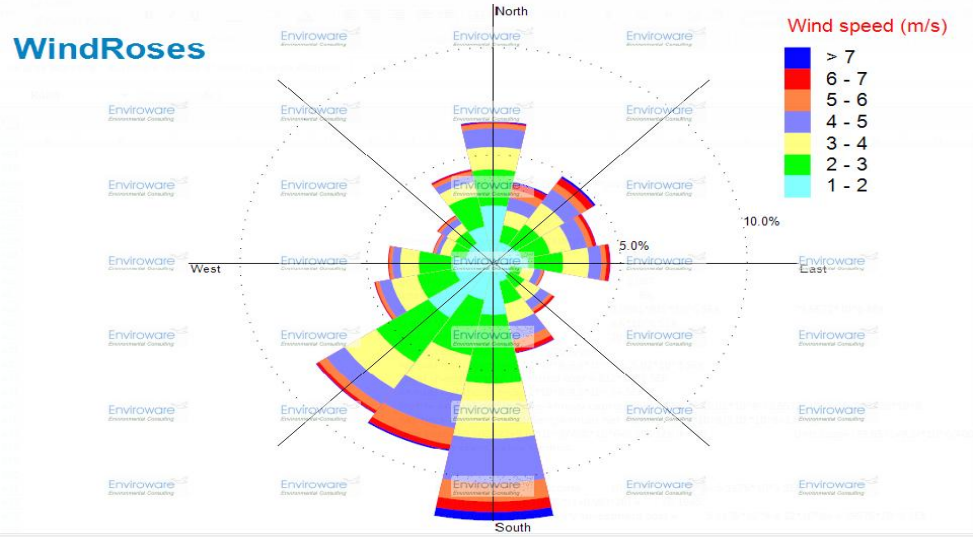

Figure 3.1: Wind Roses showing the wind direction at Stöpsjön

Now, based on wind roses as shown in figure 3.1, it is observed that the wind speed in the region of Stöpsjön (near the Karlstad municipality of Sweden) ranges from 1 m/sec to more than 7 m/sec, with a dominant direction around 180° towards South. It is also observed from the figure 3.1 that during the year of 2012, wind blew in all 16 directions but most of the time, wind blew towards south of the region.

An important thing to be noticed from the figure is that when the wind speed is above 7 m/sec, it mostly blows towards north or south of the region and does not significantly blows towards east or west of the region. Hence, based on dominant wind direction, the wind turbines were installed towards south of the region with an approximate angle of 180°. Now, for getting an actual look of the wind farm, a sketch was made with the help of Google Earth© indicating the location and direction of installed wind turbines and is shown in figure 3.2.

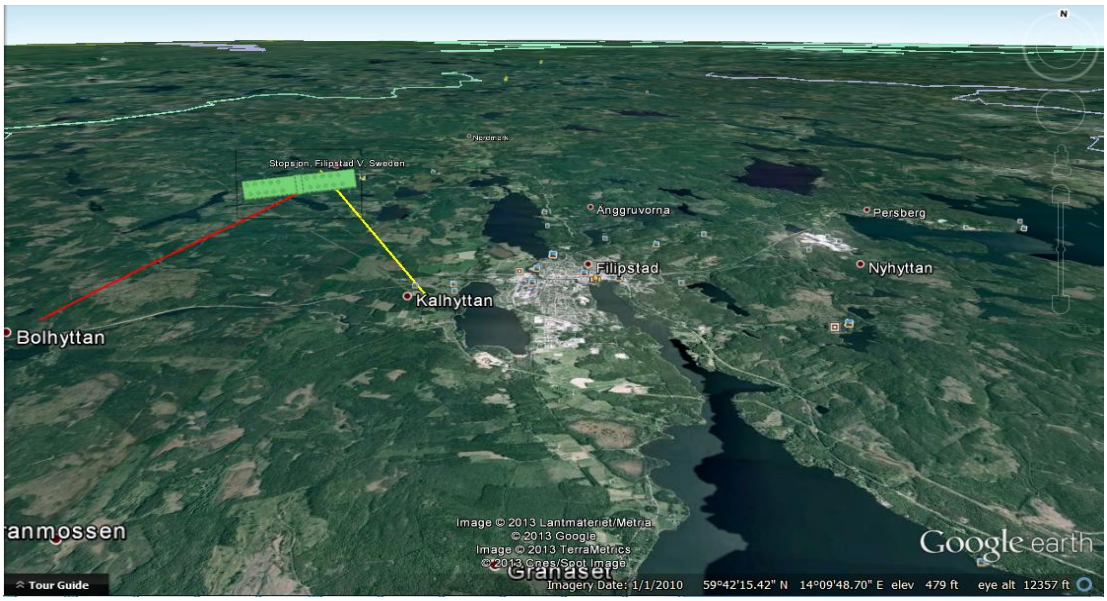

Figure 3.2: Google map showing the location of wind farm

In figure 3.2, the first line indicates 180° direction towards South from Stöpsjön to Bolhyttan, whereas, the second one indicates a distance of about 10 km between Stöpsjön and Kalhyttan. Moreover, this distance allows the wind power connection at Stöpsjön to get integrated with a 130 kV regional grid (Kalhyttan). Now, keeping this direction into consideration, two fields of a wind farm were drawn; each of these fields consists of 10 wind turbines.

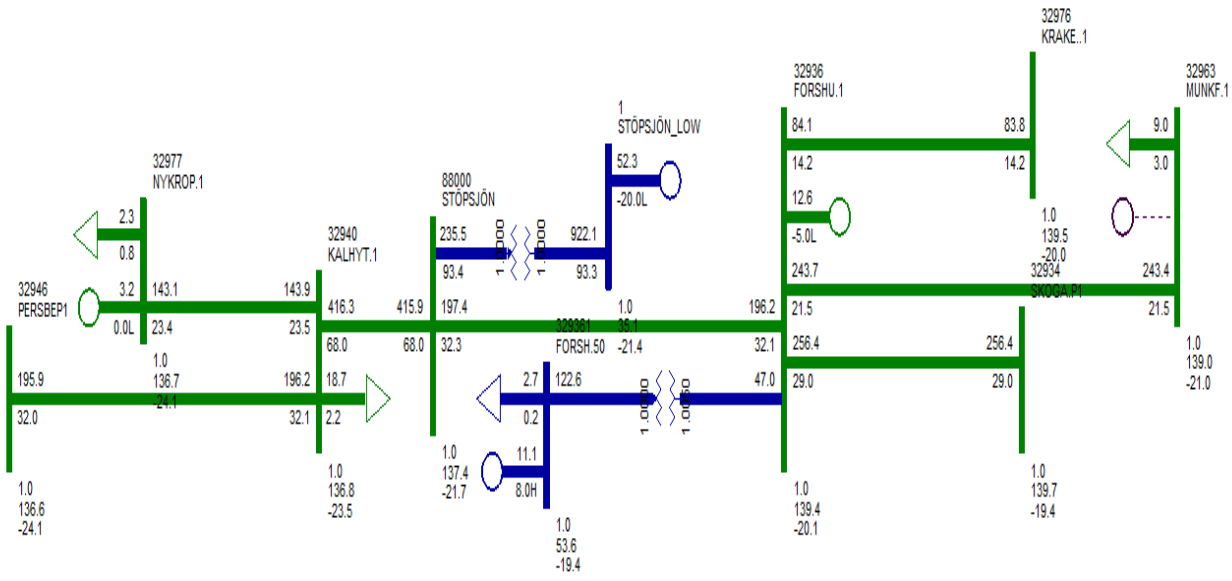

Figure 3.3: Wind power modeling in PSS/E©

Figure 3.3 shows modeling of the wind farm with an installed capacity of 60 MW in PSS/E©. This wind farm is connected in between of Forshult (bus no. 32936) and Kalhyttan (bus no. 32940) buses. Now, for integrating the wind power at Stöpsjön with the regional network of Fortum Distribution AB, the voltage at wind farm (34.5 kV approx.) must be identical with the grid voltage (135 kV approx.) to get synchronized with the system. Hence, in this regard, there is installed a step-up transformer between the wind park and the network connection that increases the voltage from 34.5 kV to 135 kV.

Moreover, Enercon E-101 wind turbine is used in this project in terms of providing a required amount of electric power (a maximum of 60 MW). The diameter of this turbine is 101 m; hence an optimal distance between 20 wind turbines is chosen in such a way that low wake, low noise and smaller interference effects should be observed. Based on these criteria, an optimal spacing is chosen amongst the turbines so that even at low wind speeds, a sufficient power is obtained. Now, in this project, it is assumed that a 7 rotor diameter distance is useful between the turbines located towards the main wind direction, while a 6 rotor diameter distance is optimum for the wind turbines facing an orthogonal wind direction [12], i.e.

- Main wind direction distance: 707 m
- Orthogonal wind direction distance: 606 m

Moreover, the main wind direction distance is a horizontal distance amongst the turbines installed in two different rows. The turbines installed in these rows experience the front direction of the wind speed [12]. Similarly, the orthogonal wind direction distance shows a vertical distance amongst the turbines installed in a same row [12]. Furthermore, the turbines installed in this path experience the wind speed in an orthogonal direction. Now, based on the aforementioned distance between the installed wind turbines, the total area of the wind farm will be:

Field 1 or 2:

Width: 707 m

Length: 2424 m

Area: 1.717 km^2

Total Area (Field 1 and 2): 3.427 km^2

Both fields are assumed identical in size, with total area equal to 3.427 km^2. Moreover, the length of each field is found almost three times to its width.

3.2 Wind Power Generation

Besides selecting a suitable location for installation of the wind turbines, their connection with the regional grid is another important factor to be taken into consideration. Connecting the wind turbines with the grid is a complex issue due to an unstable nature of the wind power. Now, before connecting the wind turbines with regional grid, following issues from a general perspective must be addressed properly [22].

- Due to difficulties involved in predicting the wind power production, the operation of power system can get affected to a significant extent
- A considerable impact of wind inconsistency on system operating costs
- Power imbalance issues in case of more wind power generation than required or vice versa
- Power quality problems in terms of voltage dips and frequency variations
- A need of reliable transmission planning for allowing the electric power from generation sources towards the load points

Now, in this project for obtaining the required (requirement set by DSO) amount of wind power generation, an installment of 20 Enercon E-101 wind turbines was taken into account. An area of 3.427 km^2 was allotted for installation of these turbines. Moreover, each Enercon E-101 wind turbine can produce a maximum of 3 MW of electric power based on its maximum allowable wind speed; whereas, when this wind speed is crossed and reaches at cutout speed of the turbine, the turbine gets stopped from working.

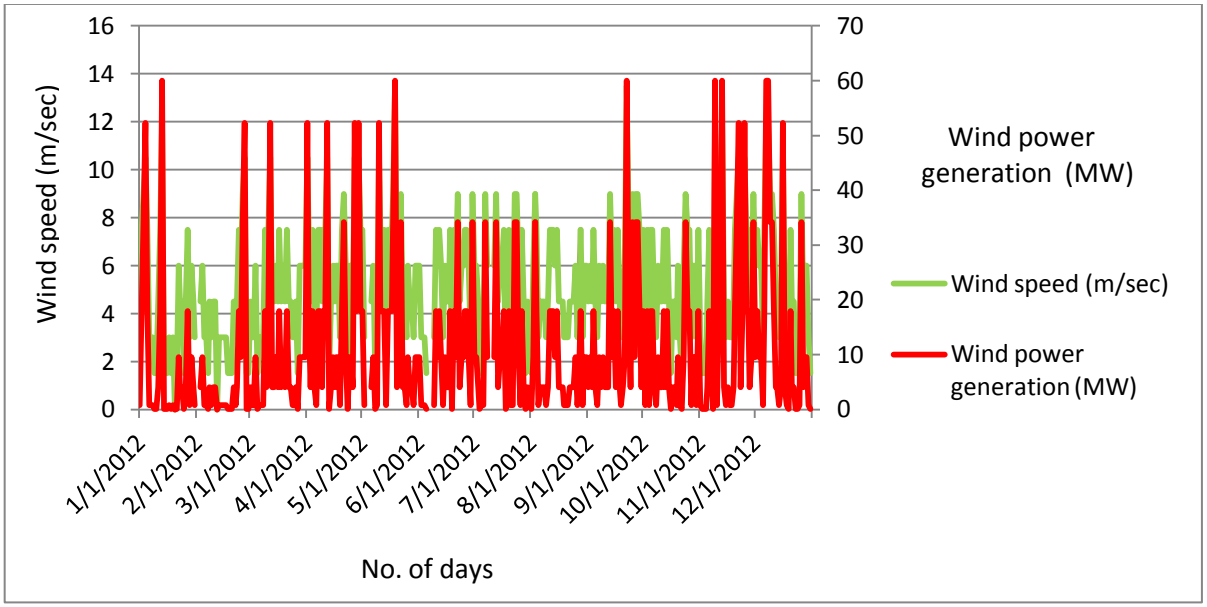

Figure 3.4: Wind Speed versus Power Generation

Now, based on the figure 3.3, it is evident that the maximum wind speed at 100-110 meters of hub-height was obtained around 14 m/sec with lowest one around 1.5 m/sec. Another important thing to be noted from the graph is the trend of wind speeds with respect to variations in the seasons. Similarly, the average wind speed during the whole year is observed around 6 m/sec that is remarkable on the other side.

3.3 Wind Energy Output

The wind power is not only significant in terms of fulfilling the growing demand of electricity but is also useful in terms of making the environment free from pollution [6]. Now, for getting the maximum amount of electricity from the wind power as well as making sure that the wind turbines are able to generate the required amount of electric power; following factors [12, 22] must be considered before head:

- Selection of long rotor turbine blades helps in giving the maximum wind energy output
- An increment in hub-height leads to increase the energy output yield
- A higher load demand during the windy periods helps in the increase of energy yield and makes the turbines not being stopped forcefully
- The installation of wind turbines in the windy regions may help in the export of electricity if its local consumption is low; giving significant profits
- With increase in size of the wind turbines and hence that of the wind farm (based on the wind power production), the cost of electricity per kWh may decrease a lot

Now, two important tools are required for calculating the annual electricity output, i.e. power curve of the wind turbine and annual frequency distribution of the wind speeds at the projected wind farm site. Both of these factors may help in giving an exact amount of electricity that a wind turbine can generate when installed at the given site [12].

Basically, a power curve is some sort of a tool that gives an idea regarding electric power, a wind turbine is expected to produce at different wind speeds [12]. Whereas, the frequency distribution is a tool that gives information regarding wind speeds at a site where the wind turbines are supposed to be installed as well as it also helps in providing information of how many hours a year; the wind will blow at a certain wind speed [12].

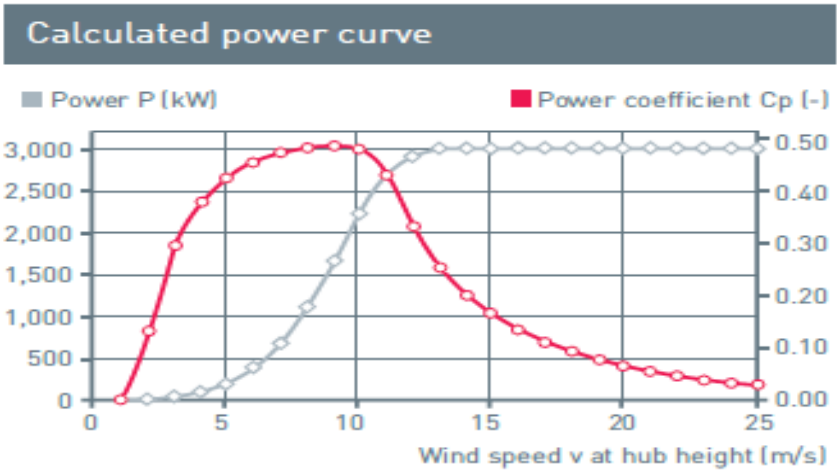

Figure 3.5: Power Curve of Enercon E-101 Wind Turbine [23]

Based on the power curve as shown in figure 3.5, it is evident that the cut-in speed of E-101 wind turbine is around 3 m/sec, i.e. when the turbine starts to generate electricity. Moreover, it indicates that the turbine is able to generate maximum (nominal) output power, when it experiences wind speed around 12 m/sec. Now, after considering the power curve of E-101 wind turbine, frequency distribution of wind speeds in an area nearby the location of wind farm at Stöpsjön, Sweden was calculated, based on the year of 2012 and is shown in table 3.1.

Table 3.1: Annual frequency distribution of wind speeds

Wind Speed Intervals (m/sec)	Frequency Distribution (%)	No. of hours/year	Calculated Power (MW)
0-0.75	8.70	762	0
0.75-2.25	14.75	1296	0.03
2.25-3.75	22.48	1975	0.74
3.75-5.25	21.07	1851	4
5.25-6.75	14.98	1316	9.58
6.75-8.25	10.35	909	19.90
8.25-9.75	4.57	402	34.20
9.75-11.25	2.27	200	52.30
11.25-12.75	0.57	50	60
12.75-14.25	0.24	21	60
> 14.25	0.02	2	60

Now, based on table 3.1, it is evident that 2.25-3.75 m/sec is a dominant wind speed interval at 100-110 meters of hub-height. Similarly, the next dominant wind speed interval in the vicinity of wind turbines ranges in between of 3.75-5.25 m/sec. Moreover, a frequency distribution of the wind speed interval ranging in between of 6.75-8.25 m/sec is also noted significant during the year of 2012.

Furthermore, in case of wind speeds higher than 12 m/sec, a single E-101 wind turbine is able to produce the maximum electric power of about 3 MW. Similarly, based on the table 3.1, it is also observed that maximum electric power of about 60 MW can be achieved for about 73 hours during a single year of 2012. Now, based on information from figure 3.4 (the power curve) and table 3.1 (frequency distribution), the annual electricity production from 20 E-101 wind turbines will be:

$$Annual\ Production\ =\ (0.03 * 1296) + (0.74 * 1975) + (4 * 1851)\ \ldots$$

$$\ldots + (9.58 * 1316) + (19.9 * 909) + (34.2 * 402) + (52.3 * 200) + (60 * 50)$$
$$+ (60 * 21) + (60 * 2) = 68.19\ \text{GWh}$$

Due to variations in the expected wind speeds, the annual energy production of the wind farm may differ from the calculated value. Moreover, the wake effect may also influence on the output wind energy production and hence may reduce the output electric power. Now, based on frequency distributions as shown in table 3.1, it is observed that due to zero wind speed, the wind turbines remain quit for about 8.7% of the total time in the year of 2012. Now, the annual electricity production from a 60 MW wind farm can be 68.19 GWh, if the wind turbines run for a maximum of 8020 hours out of 8784 hours. Moreover, besides variations in the wind speed, the other factors must be taken into account as well that may have a significant impact on the wind energy production.

Amongst these factors, the crucial ones are the maintenance work and the ice falling on the wind turbine blades. That is, the wind turbines cannot operate when there is a severe ice falling across their blades and also when they are exposed to maintenance work. Hence, based on these conditions, the actual value of the wind energy production may differ from the calculated one. Now, considering that a typical time required for routine and non-routine maintenance work is around 80 hours per year for a modern wind turbine [24]. Hence, based on a period of no wind availability and the time dedicated to maintenance work, the availability of Enercon E-101 wind turbines will be around 90.41%. Now, based on this availability of the installed wind turbines, the actual wind energy production from a 60 MW wind farm (at Stöpsjön) will be around 61.65 GWh during the single year of 2012.

CHAPTER 4

Dynamic Line Rating

The technique of determining the real time transmission line rating based on ambient weather conditions is discussed in this chapter, followed by the results obtained with the help of simulation tools.

4.1 Weather based Dynamic Rating

4.1.1 Theory

Ampacity of a transmission conductor is its ability to carry the maximum RMS (root mean square) current continuously without being deteriorated and with maintaining the safest temperature limit [25]. The overhead transmission conductors are generally classified under two different ampacity ratings, i.e.

- Static ampacity
- Dynamic ampacity

Transmission of maximum permissible current based on allowable conductor temperature is known as transmission capacity of the overhead conductors [26]. With traditional Static Line Rating approach, conductor carries maximum current based on worst weather conditions [26]. This approach however, does not address the real-time information hence it limits the actual capability of OH-conductors to transmit the electric power [26].

Now, if the real-time weather based information is used in place of fixed assumptions then actual capacity of overhead lines can be obtained. The technique that employs such information is known as the Dynamic Line Rating [26]. Moreover, it is developed on the basis of equations provided in IEEE-738-2006 standard [19] and the real-time weather data [26]. Mainly, DLR is used for two purposes; first to increase the capacity of overhead conductor in terms of transmitting the maximum electric current and secondly to control the supply of electricity during peak load and emergency states [26]. For fully utilizing the capacity of overhead conductors in terms of electricity transmission, the traditional SLR approach is not suitable at all, and requires the deployment of DLR technique in the overhead transmission network to fulfill the growing demand of electricity and avoiding the costly investments involved in rebuilding or construction of new lines [17].

Now, regarding the weather effect on conductor ampacity, it is observed that in the presence of low ambient temperature and high wind speed (perpendicular to the conductor), the overhead line becomes able to carry the further loading up to its maximum capacity. To get an overall picture of the changes on conductor (VL3) ampacity based on SLR assumptions, there is drawn a table 4.1 as an example.

Table 4.1: A typical example of weather effect on line ampacity

Hawk ACSR OH-line (30 km) with SLR assumptions: 30°C, 0.6 m/sec and Day-time	
Variation in Weather Parameter (s)	**Change in Conductor ampacity**
Ambient Temperature (°C) • +5°C Variation • −5°C Variation	 • 21.7 % Decrease in Capacity • 17.7 % Increase in Capacity
Wind Speed (m/sec) at line corridor 1 m/sec Increase • 45° angle • 90° angle	 • 24.8 % Increase in Capacity • 36.9 % Increase in Capacity

The results shown in table 4.1 are calculated based on typical fixed weather assumptions, i.e. the highest ambient temperature, the lowest wind speed and the maximum solar radiation (during day-time) for a 30 kilometer long ACSR overhead conductor. Furthermore, from table 4.1, it is observed that there is a huge impact of wind speed and its direction on increasing or decreasing the conductor ampacity to a large extent as compared to changes in ambient temperature.

Meanwhile, the low ambient temperature combined with high wind speed and its direction (perpendicular to conductor's position) increase the conductor's ability significantly; in terms of enabling it to carry maximum electric current without being overheated and/or violating the safe ground clearance requirements. Now, based on relationship between ambient temperature (°C) and solar radiation (W/m^2), there is shown a figure 4.1, illustrating the relationship among these weather parameters for the whole year of 2012 during a particular hour of the day (between 7 am to 19 pm).

4.1.2 Results

Now, here in this section, the correlation between ambient temperature and the solar radiation based on the year of 2012 is shown in general. However, the detailed analysis of the results between ambient temperature and the solar radiation for each month of the year 2012 is shown in appendix A.

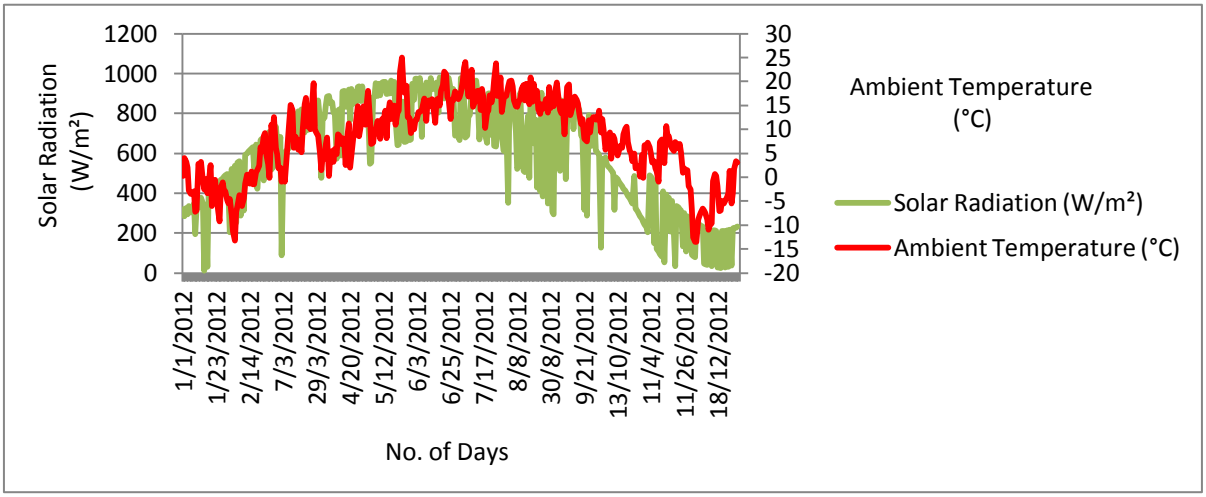

Figure 4.1: Solar Radiation (W/m^2) versus Ambient Temperature (°C) in 2012

4.2 Line Current

4.2.1 Theory

Line current represents the flow of current through a conductor during normal state of the power system. In this project, line current was changed by varying the loads situated in area 160 of the 130 kV sub-transmission network to check stress on 'VL3' overhead conductor. After variations in the system loads and by addition of wind power generation; the current and temperature across 'VL3' overhead line were analyzed. Furthermore, it was calculated with the help of PSS/E© (power system simulation) software.

The area 160 belongs to Värmland regional network of Fortum Distribution AB and is located in the western (mid-south) part of Sweden. The operational voltage of this network is 130 kV and mostly covers the industrial loads with some residential loads as well. Initially, this network was built by several large industries (paper and steel) during mid of the last century but after exploitation of hydro power in the region, the network was expanded. Now, in the north of this network, there exists huge hydro power generation whereas its south is dominated by several loads. Hence, this network connects the electric power generation from north with the loads in its south.

Besides, connections with local generation, the network is also connected with other network owners as well, for example having connection with Norway (west of the Värmland regional network) and with Vattenfall (southwest of the Värmland regional network). The import and/or export of electricity is done via a connection at Charlottenberg. Moreover, the network is also connected with Swedish national grid via two 400 kV-stations in Borgvik (west of Karlstad) and Lindbacka (west of Örebro).

Now, the 'VL3' overhead line was constructed to connect huge electricity generation around west of the network with its demand in the east. Hence, in this regard, the conductor VL3 connects west of the network with its east. Moreover, in the east of VL3 overhead line, there exists a connection with the transmission grid as well. Now, based on this connection, the electricity flows from west to east of the line. The figure 4.2 further explains the connections of VL3 in Värmland regional network.

Figure 4.2: Connection of VL3 in the Värmland regional network

The total load connected in Värmland regional network is around 910 MW; however, during the whole year of 2012, net power demand in the regional network was observed significantly lower in comparison to the full load power demand. Therefore, based on high generation (west of VL3) and low demand (east of VL3) of electricity, the VL3 overhead conductor remains periodically highly loaded/stressed. Now, the possible solution for reducing stress across this overhead conductor can be either replacing it with another conductor or applying the dynamic line rating approach across it. The former solution is not only cheaper but can be implemented within a fraction of the time required for a new line construction as well [27]. Now, based on net power demand in the Värmland regional network during each month of year 2012, there is drawn a pie chart, illustrating monthly percent based net power demand with respect to maximum power demand of the total load connected in the network.

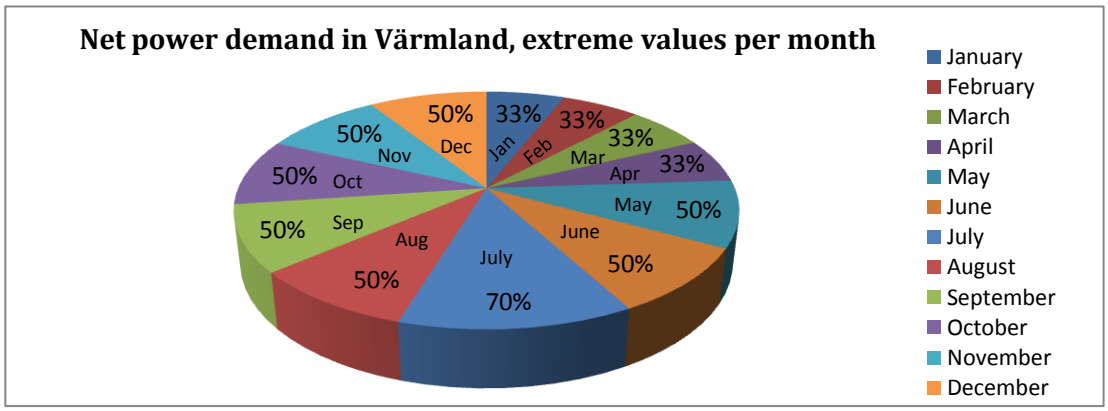

Figure 4.3: Net monthly power demand in Värmland regional network

From figure 4.3, it is observed that during summer, power demand in the network is comparatively lower than in the winter. The lowest power demand is observed in July with 70% load remained switched off.

4.2.2 Results

According to figure 4.3, the net power demand during summer remains comparatively lower than in case of winter. The reason could be high heating demand during winter that on the other hand does not exist during summer timings in Sweden. Now, based on net power demand, the temperature across VL3 overhead conductor and the current flowing through it were calculated and are shown in figure 4.4.

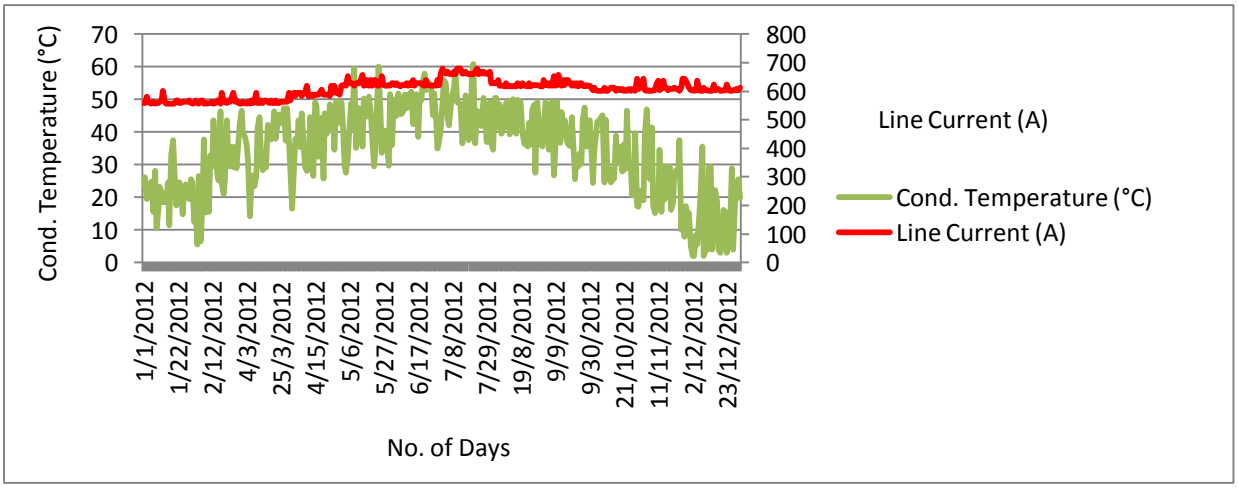

Figure 4.4: Line Current (A) versus Conductor Temperature (°C) in 2012

Based on figure 4.4, the highest conductor temperature is found around 61°C, whereas the lowest one is noted to be 3°C. This lowest conductor temperature was obtained due to minimum ambient temperature, high wind speed and the lowest solar radiation during a typical coldest day of December. Moreover, a detailed analysis of conductor temperature versus the line current for each month is shown in appendix B.

4.3. Static and Dynamic Ampacities

4.3.1 Theory

The dynamic and/or static ampacity is based upon two main factors, i.e. physical characteristics of the conductor and environmental parameters [2], with sub categories as:

- Conductor diameter
- Conductor temperature
- Ambient temperature
- Wind speed
- Angle between wind speed and conductor
- Solar radiation

4.3.2 Results

The dynamic and static line ampacities for VL3 overhead line are calculated in this section in addition to line current (based on the monthly load changes and the hourly wind power generation).

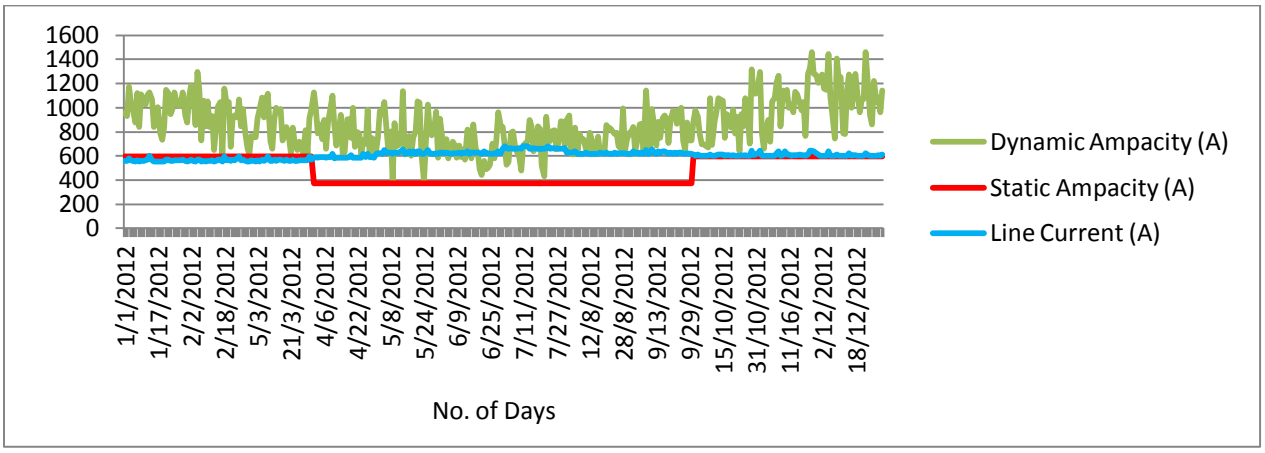

Figure 4.5: Static and Dynamic Ampacities (A) versus the Line Current (A) in 2012

Now, regarding the network operations, it is analyzed that during winter, the dynamic and even the static line ampacity is sufficient to meet the load demand but during summer timings, the situation gets different. During peak summer days, it is observed that the line current gets increased than the dynamic line ampacity, whereas during rest of the days in the year, the dynamic ampacity is observed more than enough to meet the load demand. Moreover, the correlation amongst dynamic ampacity, static ampacity and the line current during each month of the year is shown in appendix C.

Chapter 5

Economic Analysis

Issues related to conducting an investment analysis of the proposed wind farm and performing the economic study of dynamic line ratings approach are some important tasks covered in this chapter.

5.1 Introduction

Based on technological advancements in the wind energy sector, cost of electricity produced from the wind power is significantly reduced, one seventh of the electricity cost than in early eighties [22]. For carrying out the economic analysis of the wind power system, it should be checked that whether this project from an economical perspective will be profitable (even on short term basis) or not. The decision making plays a vital role in this regard and needs to take into account the interest of all the involved stakeholders. From a wind farm owner's perspective, the economic analysis of wind power generation involves three main categories of economic costs [28], i.e.

- Capital costs related to construction of the wind farm
- Fixed operation costs
- External costs of the wind power generation (termed as the leakage costs)

Now, in this project, besides wind power analysis, the dynamic line rating approach is also taken into account, hence, it becomes necessary to carry out the economic analysis of dynamic line rating into consideration as well. Based on real-time DLR approach, an increase in conductor's physical capacity for transmitting the maximum electric power may yield an improvement in terms of increased flow of energy.

Hence, based on increased flow of energy, the cost of electricity may get reduced, that on the other hand may be helpful in terms of attracting many customers. It can be considered an added advantage for a utility besides saving the money from having postponed the rebuilding of existing line(s) or the construction of a new line(s) on short or long term basis. Moreover, this delay in such heavy investments may help in enhancing the effectiveness of spent money [29]. Now, from a DLR perspective, a lot of financial benefits can be directly or indirectly achieved [29], for example:

- Cheaper electricity for consumers (a DLR advantage for the society)
- Better prices for the wind power owners (in terms of lower connection fee)
- Improvement in economical usage of transmission lines (useful for the DSO)
- Making the asset utilization cost effective (valuable from a DSO perspective)

5.2 Wind power economic analysis

5.2.1 Introduction

For making the wind power project profitable, it is necessary that the wind turbines are installed at a suitable location (as shown in chapter 3) to generate a sufficient amount of electricity. As, it may help in giving an enough revenue, so that the banks should be willing to offer the loans (on the condition that they will get back their money soon); similarly, it may help the utilities in getting significant returns at the cost of their huge investments [12]. The economic analysis of wind power system is classified into different categories being mentioned in the following sections.

5.2.2 Capital cost investment analysis

Capital costs are related to purchase of the wind turbines, their installation and connection with the national or regional grid [12], however in this project, the wind park is connected with regional grid of Fortum Distribution AB. In a broader perspective, the costs related to transferring the turbines from their manufacturing location to their installation site, purchase of land for the construction of wind farm, making the foundations, using the machinery to install them, lying of cables to connect the turbines with the grid and the purchase of transformers (to step up the voltage) are some important factors observed in the capital cost investment analysis [12].

Now, considering investment costs of wind power in Sweden, it is observed that the cost of a wind turbine to produce one kW of electric power is around 11,950 SEK (equivalent to 1,422 €/1,852 $, approx. at 1SEK≈0.119€/0.155$) [30]. Furthermore, figure 5.1 gives an explicit picture of wind power investments costs (obtained from the wind power book [12]), mentioning a total capital cost breakdown for a proposed 60 MW wind farm in detail.

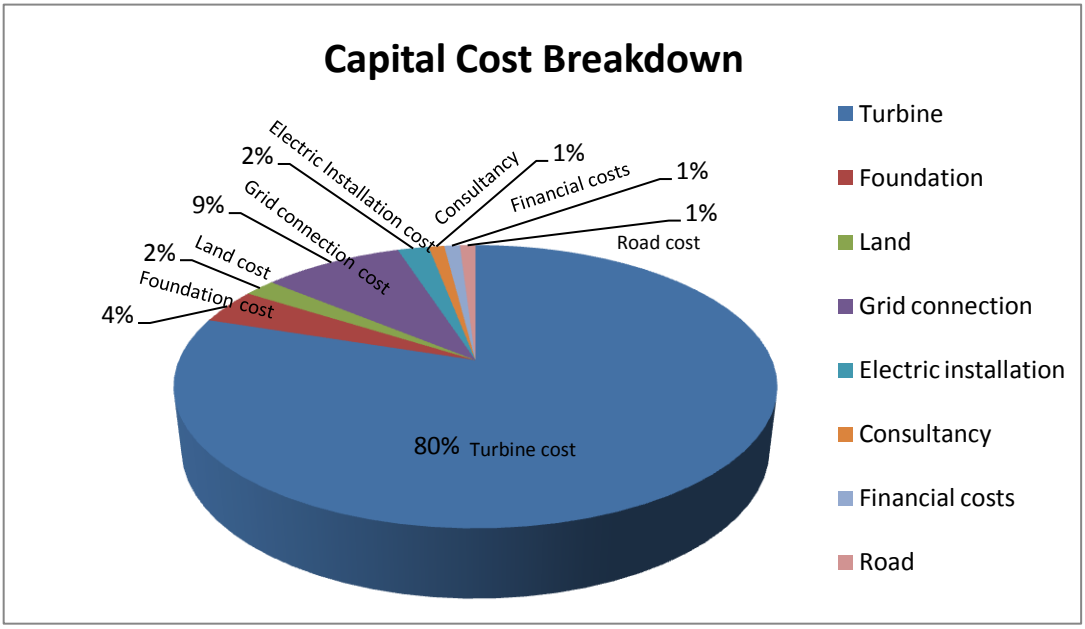

Figure 5.1: Capital Cost Breakdown of a 60 MW wind farm at Stöpsjön

Based on percentage breakdown of capital costs (as shown in figure 5.1) involved in the construction of a 60 MW wind farm at Stöpsjön, the detailed figures in MSEK are shown in table 5.1, i.e.

Table 5.1: Investment Cost of Wind farm at Stöpsjön

Category	Capital Cost (MSEK)
Wind Turbines	717
Foundation	35.8
Land	17.9
Grid Connection	80.6
Electric Installation	17.9
Consultancy	8.9
Financial Costs	8.9
Road	8.9
TOTAL	896

The electric installation cost in table 5.1 belongs to the expenditures in terms of laying the cables for facilitating the electric power from wind turbine to a step up transformer [12]. Similarly, the grid connection cost belongs to expenditures related to purchase of the transformer and the connection of wind farm with regional grid (the price may vary depending upon the equipments, the location and nature of the projects) [30]. Moreover, based on the same table, it is also observed that the total capital cost from acquiring the land for a 60 MW wind farm at Stöpsjön to its connection with the regional grid will be 896 MSEK (106.5 M€/138.5 M$, approx. at 1SEK≈0.119 €/0.155 $).

5.2.3 Operation and Maintenance cost analysis

Operation and maintenance costs belong to the expenditures related to service, insurance and administration for handling the proper operation of installed wind turbines [12]. The service costs are related to overhauling and examination of wind turbines in terms of checking their regular operating status. Similarly, the insurance is also necessary; particularly when warranty of the wind turbines is expired, as well as it may be helpful in terms of covering the fire or any other accidents [12].

The administration cost is also required in case of paying the municipality taxes and covering the telephone bills [12]. Moreover, the table 5.2 gives a detailed overview of annual operation and maintenance costs (in MSEK) required for a 60 MW wind park project at Stöpsjön, Sweden.

Table 5.2: Annual O & M Costs of the Wind farm at Stöpsjön

Category	Costs (MSEK)
Service	2.4
Insurance	2.4
Measurement	0.42
Telephone	0.12
Taxes	1.92
Fees	0.06
Administration	0.3
TOTAL	7.62

5.2.4 Revenue

Revenue is obtained after selling electricity produced from the wind farm on annual basis. Now, for annual revenue or income, the cost of electricity was obtained from the nord pool spot [31]. Similarly, the information regarding green certificate price in Sweden was obtained from 'Svenska Kraftnet' [32]. Now, from a 60 MW wind farm (at Stöpsjön), the following annual revenue was obtained.

$$Electricity\ price\ = 0.369\ \ SEK/kWh$$

$$Green\ Certificate = 0.2\ \ SEK/kWh$$

$$Annual\ Production\ = 68.19\ \ GWh$$

$$Annual\ Revenue\ = 25.16\ \ MSEK$$

5.3 Economic analysis of ampacity upgrading methods

5.3.1 Introduction

On the basis of real time information, the DLR approach helps overhead conductors to be operated safely with increased reliability. By adopting the dynamic rating approach, the capacity of overhead conductor is increased to a significant extent, allowing the transfer of electric power overwhelmingly [17]. Based on maximum allowable capacity of overhead conductor on the basis of DLR approach for transmission of huge amount of electric power, the option of replacing existing conductor with a high temperature sustaining conductor or to construct a new line in parallel of existing conductor to transfer the required amount of electric power seems inappropriate from economical, environmental and social perspectives [29].

The dynamic thermal line rating enables the power system operators in terms of making judgments regarding the actual thermal limits of overhead lines (based on maximum flow of current) hence, in this way, the operators may take opportunities for delivering more power during its peak demand and avoiding unnecessary load shedding in case of contingency [33]. Now, based on this fact, the electric power not only can be transferred reliably but also unnecessary load shedding can be avoided, and ultimately, the utility may get saved from financial losses. Similarly, the power capacity limitations for any utility can be expensive as well, whereas, with a small increase in capacity of the overhead lines, the utility may earn huge profits [33].

Now, in following sections, annual revenue based on increment in capacity of an existing conductor (VL3) with the help of DLR technique is taken into account and then the annual revenue based on increment in the capacity of a new overhead conductor (area 593mm²) with the help of conventional ampacity upgrading technique (SLR) is calculated. At the end, the economic value of postponing the costly power system investments will be taken into account as well.

5.3.2 Net annual Income based on DLR approach

The dynamic ampacity in this project was calculated for the whole year of 2012 and was based on a particular hour of the day. The selection of that hour was assumed as random and was chosen in between of a 13-hour range (7 am to 19 pm). Now, based on this ampacity rating, the allowed energy flow E_d during the selected hour was calculated for the whole year of 2012 and is given as:

$$E_d = 38.51\ GWh/year$$

Similarly, based on static ampacity rating, the allowed energy flow E_s (for single hour in a day) through 'VL3' overhead line for the whole year of 2012 was calculated as:

$$E_s = 21.68\ GWh/year$$

Now, from the above figures, it is observed that the energy flow through 'VL3' OH-line on the basis of dynamic ampacity is noted around 1.8 times higher in comparison to its flow on the basis of static ampacity through the same overhead line. Moreover, the allowed energy flow E_{s1} (during single hour of the day) through the new planned overhead conductor of area 593 mm² based on its static ampacity (63% to that of existing conductor) during the whole year of 2012 is found around 35 GWh/year, i.e.

$$E_{s1} = 35.37\ GWh/year$$

Furthermore, applying the real-time dynamic rating technique across an existing overhead conductor requires equipping the line with useful communication and computer tools for transferring the real-time data from the line corridor to the control room. The different monitoring and communication tools are available in this regard; CAT-1 transmission line monitoring system is one of them [27].

Now, if these tools are installed across an existing overhead conductor for continuous real-time monitoring and transmission of data to the utility's control centre then it costs around 200,000 $ (one time product cost estimation) for a single existing transmission line conductor (excluding the shipment, installation and O&M costs) [27]. Now converting it to SEK (1 SEK≈0.15 $), the expenditure D_e will be equivalent to:

$$D_e = 1.317 \ MSEK$$

With the help of DLR technique, the transfer of electricity through existing overhead conductor is observed significantly higher than its flow based on traditional SLR approach. Hence, the energy that is curtailed by SLR approach can be transferred with the help of DLR technique across the same overhead conductor. Now, the transfer of energy through VL3 overhead line being curtailed by SLR approach $E_{c,SLR}$ was allowed to be transferred with the help of DLR technique and is found as:

$$E_{c,SLR} = 16.83 \ GWh/year$$

Now, the net annual income I_d based on this allowed energy flow at an assumed electricity price (λ) of 0.369 SEK/kWh [31] for the year of 2012 will be:

$$I_d = E_{c,SLR} * \lambda - D_e = 4.89 \ MSEK$$

Furthermore, due to involvement of different stakeholders in the electricity market, it is difficult and complex to estimate the income or profit for each involved stakeholder, i.e. how much share should be allocated for the wind power owners, the utilities and the DSOs when the energy is transferred based on DLR approach (particularly due to its dynamic nature). Hence, to avoid such assumption based profits or incomes for each stakeholder, it is better to focus on the economic analysis based on the benefit of capacity increase across an overhead line. Now, this financial benefit after implementation of DLR approach across the existing overhead line (VL3) is calculated as:

$$\frac{I_d}{E_{c,SLR}} = 0.29 \ MSEK/GWh$$

From the above figure, it is observed that based on DLR approach, an increment of 1 GWh energy flow through existing overhead line (VL3) may yield a benefit of 0.29 MSEK during a single year. Hence, the higher the increase in the conductor capacity (for transmitting the electricity) the higher will be the financial benefit.

5.3.3 Net annual Income in case of upgrading the line

Replacement of the existing line 'VL3' with a new conductor that has an area of 593 mm^2 and the length of 30 km will require an approximate total capital cost $C_{u,t}$ of:

$$C_{u,t} = 32.1\ MSEK$$

Now, assuming that the cost related to upgrading the conductor is financed by a loan at a nominal interest rate of 7.5% (real interest rate + expected inflation) and the loan is required to be paid in the period of 20 years then based on this data, the capital cost of upgrading the conductor on annual basis $C_{u,a}$ can be calculated with the help of annuity method. Moreover, in this method, the value of annuity (based on pay-back period and the interest rate) can be calculated with the help of equation 5.1 [12], i.e.

$$a = \frac{r * (1+r)^n}{(1+r)^n - 1} \tag{5.1}$$

where, a is the annuity, r is the nominal interest rate, and n is the pay-back period in years

Now, based on equation 5.1, the annuity will be:

$$a = \frac{0.075 * (1+0.075)^{20}}{(1+0.075)^{20} - 1} = 0.097$$

After calculation of annuity, the annual capital cost of replacing the existing overhead conductor (VL3) with a new overhead conductor (of area 593 mm^2) can be calculated with the help of equation 5.2 [12], i.e.

$$C_{u,a} = a * C_{u,t} \tag{5.2}$$

$$C_{u,a} = 0.097 * 32.1 * 10^6 = 3.11\ MSEK$$

After replacement of existing conductor with a new OH-line that has 1.1 times larger cross-sectional area, the transfer of electricity (based on SLR approach) through this new overhead line gets increased significantly as compared to its flow through the existing smaller cross-sectional area OH-line. Moreover, the energy (based on static ampacity) that is curtailed by existing conductor $E_{c,VL3}$ can be transferred through the new overhead line and is given as:

$$E_{c,VL3} = 13.69 \ GWh/year$$

$$\lambda = 0.369 \ SEK/kWh$$

$$I_{u,a} = E_{c,VL3} * \lambda - C_{u,a}$$

or,

$$I_{u,a} = 13.69 * 0.369 - 3.11 = 1.94 \ MSEK$$

where, λ is the current electricity price and $I_{u,a}$ is the net annual income after the line upgrading

Now, the economic analysis related to increase in conductor capacity when the existing overhead line is upgraded with a new overhead conductor with aforementioned specifications will be as:

$$\frac{I_{u,a}}{E_{c,VL3}} = 0.14 \ MSEK/GWh$$

Based on this value, it is observed that after the upgrading of existing conductor, an increment of 1 GWh energy flow through the new overhead line may yield a benefit of 0.14 MSEK during a single year.

5.3.4 Net annual Income in case of building a new line

Considering that an approximate total capital cost $C_{n,t}$ associated with building a new overhead line of about 30 km in length with an area of 593 mm^2, designed for 130 kV operating voltage is:

$$C_{n,t} = 39.3 \ MSEK$$

Now, similar to upgrading of the line, if the construction of a new overhead conductor is financed in the form of a bank loan at the nominal interest rate of 7.5% with a pay-back period of 20 years then the annual capital cost $C_{n,a}$ calculated with the help of annuity method from equations 5.1 and 5.2 will be:

$$C_{n,a} = a * C_{n,t}$$

where,

$$a = \frac{0.075 * (1 + 0.075)^{20}}{(1 + 0.075)^{20} - 1} = 0.097$$

Hence, the annual capital cost for the new line construction will be:

$$C_{n,a} = 0.097 * 39.3 * 10^6 = 3.81 \ MSEK$$

Now, after construction of a new OH-line having 1.1 times larger cross-sectional area, the transfer of electricity (based on SLR approach) through this new overhead line gets increased to a significant extent as compared to its flow through the existing smaller cross-sectional area OH-line. Furthermore, the energy (based on static ampacity) that is curtailed by existing conductor $E_{c,VL3}$ can be transferred through the new overhead conductor and is given as:

$$E_{c,VL3} = 13.69 \ GWh/year$$

$$\lambda = 0.369 \ SEK/kWh$$

$$I_{n,a} = E_{c,VL3} * \lambda - C_{n,a}$$

or,

$$I_{n,a} = 13.69 * 0.369 - 3.81 = 1.24 \ MSEK$$

where, λ is the current electricity price and $I_{n,a}$ is the net annual income after the new line construction

Furthermore, the economic analysis related to increase in the conductor capacity when a new overhead line (with aforementioned specifications) is constructed in place of existing conductor will be around:

$$\frac{I_{n,a}}{E_{c,VL3}} = 0.09 \ MSEK/GWh$$

Based on this value, it is observed that an increment of 1 GWh energy flow through the new overhead line may yield a benefit of 0.09 MSEK during a single year.

5.3.5 Future investment analysis of postponement of line upgrading

There can be additional revenue to be earned from postponing the replacement of existing overhead conductor on a short or long term basis. Considering that if replacement of a transmission conductor is postponed for a period of 5 years (n) then based on a nominal interest rate (r) of 7.5% (real interest rate + expected inflation) with its present investment cost C_0 (related to replacing the existing 30 km long overhead conductor with 593 mm^2 conductor) around 32.1 MSEK and its future investment cost C_n equivalent to 40.1 MSEK (for example after 5 years based on 25% increase), then the net value savings based on present value of future cash flows and present value of investment cost [34] can be obtained as follows:

Now, considering the net present value as shown in equation 5.3 [34], i.e.

$$NPV = C_0 - PV \tag{5.3}$$

and, the present value as shown in equation 5.4 [34], i.e.

$$PV = \frac{C_n}{(1+r)^n} \tag{5.4}$$

Now, based on equation 5.4 [34]:

$$PV = \frac{40.1}{(1+0.075)^5}$$

or,

$$PV = 27.9 \ \ MSEK$$

Similarly, with the help of equations 5.3, and 5.4, the net value savings after having postponed the upgrading of a new line for about 5 years will be as follows:

$$NPV\ (Savings)\ = 4.1\ \ MSEK$$

where, PV is the present value and NPV is the net present value

5.3.6 Future investment analysis of postponement of new line construction

Now, considering that if the construction of a new overhead conductor (30 km long in length and 593 mm^2 in area) is postponed for 5 years then based on current nominal interest rate of 7.5% (real interest rate + expected inflation) with its present investment cost around 39.3 MSEK and its future investment cost of about 49.1 MSEK (for example after 5 years) then the net value savings based on present value of future cash flows and present value of the cost of investment [34] can be calculated as follows:

Now, from equation 5.4:

$$PV\ = \frac{49.1}{(1+0.075)^5}$$

or,

$$PV\ = 34.2\ \ MSEK$$

Similarly, with the help of equations 5.3, and 5.4, the net value savings after having postponed the construction of a new overhead line for a period of 5 years will be around:

$$NPV\ (Savings)\ = 5.1\ \ MSEK$$

5.4 Comparison amongst amapcity upgrading methods

Here, in this section, a comparison amongst different ampacity upgrading techniques is taken into account. The ampacity upgrading methods related to replacement of a smaller overhead conductor with a new larger overhead conductor and the new line construction are considered as conventional approaches for the transmission of electricity that on the other hand cannot be transferred through the old smaller overhead conductor. Now, from technical perspective, any of these conventional amapcity upgrading methods can be considered useful in terms of required electricity transmission but from an economical perspective, these methods are not feasible at all. Now, in comparison to conventional ampacity upgrading methods, it is observed that the dynamic line rating approach is not only useful from technical perspective but also feasible from economic perspective as well. Furthermore, there is drawn a table 5.3, giving an overall picture of annual benefit from the increase in conductor capacity with the help of different amapcity upgrading methods.

Table 5.3: Annual benefit from ampacity upgrading solutions

Ampacity Upgrading Solution (s)	MSEK/GWh
Dynamic Line Rating	0.29
Conductor Upgrading	0.14
New Line construction	0.09

From table 5.3, it is observed that the DLR approach is significantly profitable in comparison to conventional ampacity upgrading techniques. Furthermore, on the basis of limited information, it is difficult to find and compare the exact turnovers from the aforementioned amapcity upgrading techniques. For example, the energy transfer through conductor replacement or through a new line construction is based on static amapcity approach which may yield the predictable revenue, whereas, the revenue based on dynamic line ampacity cannot be predicted due to significant variations in the conductor capacity.

Therefore, the revenue based comparison cannot be estimated amongst static and dynamic line ratings. Moreover, the cost of dynamic rating equipments and their control room issues are also major concerns regarding the complexities in terms of making estimation of the profits obtained from the dynamic line ratings as compared to the profits based on conventional static ampacity technique. Therefore, these figures cannot be termed as reliable and may differ in terms of reality.

Chapter 6

Conclusion, Discussion and Future Work

6.1 Conclusion

In this project, dynamic line rating is implemented across an overhead line (VL3), located in a 130 kV sub-transmission system, owned by Fortum Distribution AB. Besides static and dynamic ampacity calculations, the work is also devoted to integrate a 60 MW wind park with regional grid. Furthermore, based on wind power and net electricity demand, the line current and conductor temperature are measured as well. Thereafter, a comparison amongst conductor ampacities and the line current is carried out to check that how much further the overhead conductor can be loaded up to its actual maximum capacity.

Now, based on the results of this project, it is observed that the dynamic ampacity has significantly improved conductor's capacity in terms of electricity transmission. During winter, due to low ambient temperature and minimum solar radiation, the dynamic ampacity of an overhead conductor (VL3) is found many times higher than its static ampacity. However, during peak summer days, both ampacity ratings are observed almost identical and lower than actual line current.

Furthermore, from economic study, it is observed that the ampacity upgrading of an overhead conductor on the basis of dynamic rating is significantly profitable in comparison to conductor replacement or new line construction techniques. Similarly, it is also observed that a temporary postponement of line replacement or a new line construction may also yield significant savings.

6.2 Discussion

The static line rating approach has been obsolete due to limiting the capacity of overhead lines in terms of electricity transmission, hence, the overhead conductors need to be rated based on dynamic line rating approach which on the other hand is helpful in finding their actual capacity. The conventional line rating approach not only restricts the maximum capacity of overhead lines in terms of electricity transmission but also limits the entry of renewable generation in the electricity network. Therefore, the technique based on real-time ambient conditions is required to be implemented in the power system for not only enhancing the capacity of overhead conductors but also allowing excessive renewable generation in the electricity network.

This diploma work is a step forward in this regard. In this research work, three case studies are taken into account. First case study is related to analyzing an effect of high electricity generation with low power demand on the conductor loading. The second one is related to evaluating the ampacity upgrading techniques, whereas, the third case study is devoted to performing the economic analysis of wind power system and the ampacity upgrading solutions. Finding the line loading is important in terms of checking the conductor stress on a routine basis. Furthermore, the difference between line loading and dynamic ampacity is proved helpful in terms of estimating that how much further the line should be loaded based on actual weather conditions and the load behavior during the whole year of 2012.

Now, from the results of this project, dynamic ampacity of 'VL3' overhead line is found considerably higher as compared to its static ampacity during the whole year of 2012 and is proved a useful option in contrast to traditional approach for finding the line ratings. Furthermore, regarding stress, the projected overhead conductor during summer, is observed highly loaded due to low power demand as compared to its situation in winter. Similarly, the dynamic ampacity of the same overhead conductor during peak summer timings is found insufficient in terms of required electricity transmission.

Furthermore, based on economic study results, it is observed that for transferring 1 GWh energy flow with the help of DLR approach may yield 107% more return than from the line replacement and 222% more than based on a new line construction. The same study shows that a temporary delay in line replacement or a new line construction may yield significant savings, i.e. the postponement of line replacement for 5 years may result in net savings of about 4.1 MSEK, whereas, the same delay in new line construction may provide the net savings of about 5.1 MSEK.

6.3 Future work

This project was mainly focused on connecting the wind power in a 130 kV sub-transmission grid, finding line current, and the ampacity ratings for a highly stressed overhead conductor. It also covered the economic analysis of the wind power system and the dynamic line ratings approach. Moreover, the further research can be carried out as a continuation of this diploma work to investigate the remaining issues. Following are given some important ideas that can be considered as a future research work:

- **Increasing the scope of DLR**

In this project, the technique of finding the line ampacity based on DLR was implemented on a single overhead conductor and was based on a particular day time hour (7 am to 19 pm). Now, due to its significant technical and economic advantages (as observed in this project), its usage should be extended to a large extent. It must be calculated for all those overhead lines which are assumed highly loaded (based on the observations from static line rating approach). In addition to that, for fully analyzing the DLR impact on grid operations, it must be calculated for 24 hours in a day. Not only this, but also the dynamic rating of transformers must be analyzed in response to upgrading of the line rating (based on DLR).

- **The reliability analysis**

The project did not address the reliability analysis, hence, as a future research work, it must be checked that to what extent the dynamic rating affects the system reliability. For example, considering the effect of dynamic rating on the aging of power system components in general and on transmission line conductors as particular must be taken into account. Moreover, besides these considerations, the analysis of thermal violations (particularly during emergency situations) in the presence of wind power generation should be carried out as well.

- **Control room issues**

Developing a standardized algorithm to efficiently manage the continuously varying ambient data and hence the dynamic ampacity in the control room is also a demanding future task that is required to be solved so that a reliable implementation of dynamic line rating approach should be carried out in the power system.

BIBLIOGRAPHY

[1] Thayer, Robert L., and Carla M. Freeman. "Altamont: Public perceptions of a wind energy landscape." Landscape and Urban Planning 14 (1987): 379-398.

[2] Holbert, K. E., and G. T. Heydt. "Prospects for dynamic transmission circuit ratings." Circuits and Systems, 2001. ISCAS 2001. The 2001 IEEE International Symposium on. Vol.3. IEEE, 2001.

[3] Hilber, Patrik, Carl Johan Wallnerström, Johanna Rosenlind, Johan Setréus, and Niclas Schönborg. "Risk analysis for power systems: overview and potential benefits." CIRED Workshop - Lyon (2010).

[4] "Swedish Metrological and Hydrological Institute." http://www.smhi.se (accessed on 10/12/2012)

[5] Foss, Stephen D., and Robert A. Maraio. "Dynamic line rating in the operating environment." *Power Delivery, IEEE Transactions on* 5.2 (1990): 1095-1105.

[6] Bull, Stanley R. "Renewable energy today and tomorrow." *Proceedings of the IEEE* 89.8 (2001): 1216-1226.

[7] David, Gireesh, Shobhit, Charith and Raj Kumar. "Meeting India's Renewable Energy Targets: The Financing Challenge." Climate Policy Initiative, 2012.

[8] "GWEC Global Wind Statistics 2012". Global Wind Energy Commission. www.gwec.net/wp-content/uploads/2013/02/GWEC-PRstats-2012_english.pdf, Retrieved 18 February 2013.

[9] "EU wind power capacity reaches 100GW". UPI. 1 October 2012. Retrieved 31 October 2012,http://www.upi.com/Business_News/Energy-Resources/2012/10/01/EU-wind-power-capacity-reaches-100GW/UPI-52431349087400/ (accessed on 10/01/2013)

[10] "US Reaches 50 GW of Wind Energy Capacity in Q2 of 2012". Clean Technica. 10 August 2012. Retrieved 31 October 2012, http://cleantechnica.com/2012/08/10/us-reaches-50-gw-of-wind-energy-capacity-in-q2-of-2012/ (accessed on 10/01/2013)

[11] "Wind Power." http://en.wikipedia.org/wiki/Wind_power (accessed on 29/03/2013)

[12] Wizelius, Tore. “Developing wind power projects: theory and practice.” Routledge, 2007.

[13] Baldocchi, Dennis. "Lecture 17 Wind and Turbulence, Part 2, Surface Boundary Layer: Theory and Principles." Department of Environmental Science, Policy and Management, University of California, Berkeley (2010).

[14] “Log wind profile.” http://en.wikipedia.org/wiki/Log_wind_profile (accessed on 29/03/2013)

[15] Söder, Lennart, and Mehrdad Ghandhari. "Static Analysis of Power Systems." Electric Power Systems, Royal Institute of Technology, Stockholm, Sweden (2004).

[16] Saadat, Hadi. “Power system analysis.” Singapore: WCB/McGraw-Hill, 1999.

[17] S.D. Kim, and M.M. Morcos, “An Application of Dynamic Thermal Line Rating Control System to Up-Rate the Ampacity of Overhead Transmission Lines.” Power Engineering Letters. *IEEE TRANSACTIONS ON POWER DELIVERY* 28.2 (2013): 1231.

[18] Merrell, John, Tacoma Power, Mike P. Diedesch, and Jared R. Johnson. "Dynamic Line Ratings for the Cowlitz-LaGrande Transmission Lines." Washington State University, 2008.

[19] IEEE, “Standard for calculating the current-temperature of bare overhead conductors,” IEEE Std 738-2006 (Revision of IEEE Std 738-1993), pp. c1–59, 30 2007 Conductors. New York. 1993.

[20] Special Course Report. “Natural Convection.” Section of Electric Power Engineering, Technical University of Denmark, 2005.

[21] Blaabjerg, Frede, et al. "Power electronics in wind turbine systems." *Power Electronics and Motion Control Conference, 2006. IPEMC 2006. CES/IEEE 5th International*. Vol. 1. IEEE, 2006.

[22] Georgilakis, Pavlos S. "Technical challenges associated with the integration of wind power into power systems." Renewable and Sustainable Energy Reviews 12.3 (2008): 852-863.

[23] Enercon: "Enercon Product Overview." E-101 Wind Turbine. http://*www.enercon.de/p/downloads/ENERCON_PU_en.pdf* (accessed on 20/02/2013)

[24] European Wind Energy Association. *Wind Energy-The Facts:" A Guide to the Technology, Economics and Future of Wind Power"*. Routledge, 2009.

[25] Williams, Noel, and Jeffrey S. Sargent. *NEC Q & A: Questions & Answers on the National Electrical Code*. Jones & Bartlett Learning, 2007.

[26] Kim, Dong-Min, et al. "Prediction of dynamic line rating based on assessment risk by time series weather model." *Probabilistic Methods Applied to Power Systems, 2006. PMAPS 2006. International Conference on*. IEEE, 2006.

[27] Seppa, Tapani O. "Reliability and real time transmission line ratings." *Nexans, Ridgefield* (2007).

[28] Deutsche Gesellschaft für Technische Zusammenarbeit (GTZ) GmbH. "Feasibility Study for Wind Park Development in Ethiopia and Capacity Building." Mesobo-Harena Wind Park Site. *Final Report, 2006.*

[29] Sandy K. Aivaliotis. "Dynamic Line Ratings for optimal and reliable power flow, enhanced power flow for the smart grid." The Valley Group, a Nexans company, FERC Technical Conference, 2010.

[30] [IRENA] - International Renewable Energy Agency, "RENEWABLE ENERGY TECHNOLOGIES: COST ANALYSIS SERIES." Volume 1: Power Sector, Wind Power, June 2012.

[31]Nord Pool Spot, April 2013. "Elspot prices (EUR/MWh)." http://www.nordpoolspot.com/Market-data1/Elspot/Area-Prices/ALL1/Hourly/ (accessed on 17/04/2013)

[32] Svenska Kraftnet, April 2013. "Green Certificate price (EUR/MWh)." http://elcertifikat.svk.se/cmcall.asp?service=CS_Reports.GetCertificates&styleFN=reports/xsl/certificates.xsl&generalpageid=2 (accessed on 08/04/2013)

[33] Douglass, Dale A., et al. "Dynamic thermal ratings realize circuit load limits." Computer Applications in Power, IEEE 13.1 (2000): 38-44.

[34] Prof. Beatriz de Blas. "Lesson 1. Net Present Value." Universidad Autonoma De Madrid, April 2006.

APPENDIX A

Solar Radiation (W/m^2) versus Ambient Temperature (°C)

For year 2012, the weather based ambient data used to calculate the dynamic line ratings is shown in this appendix:

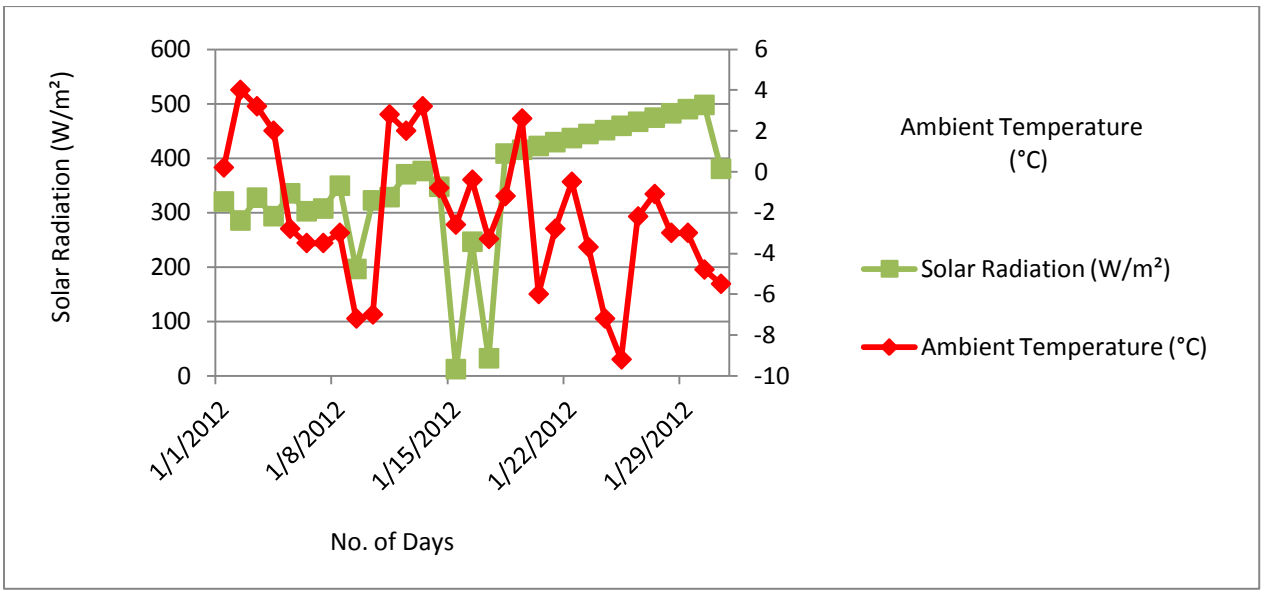

Figure A.1: Solar Radiation (W/m^2) versus Ambient Temperature (°C) in January

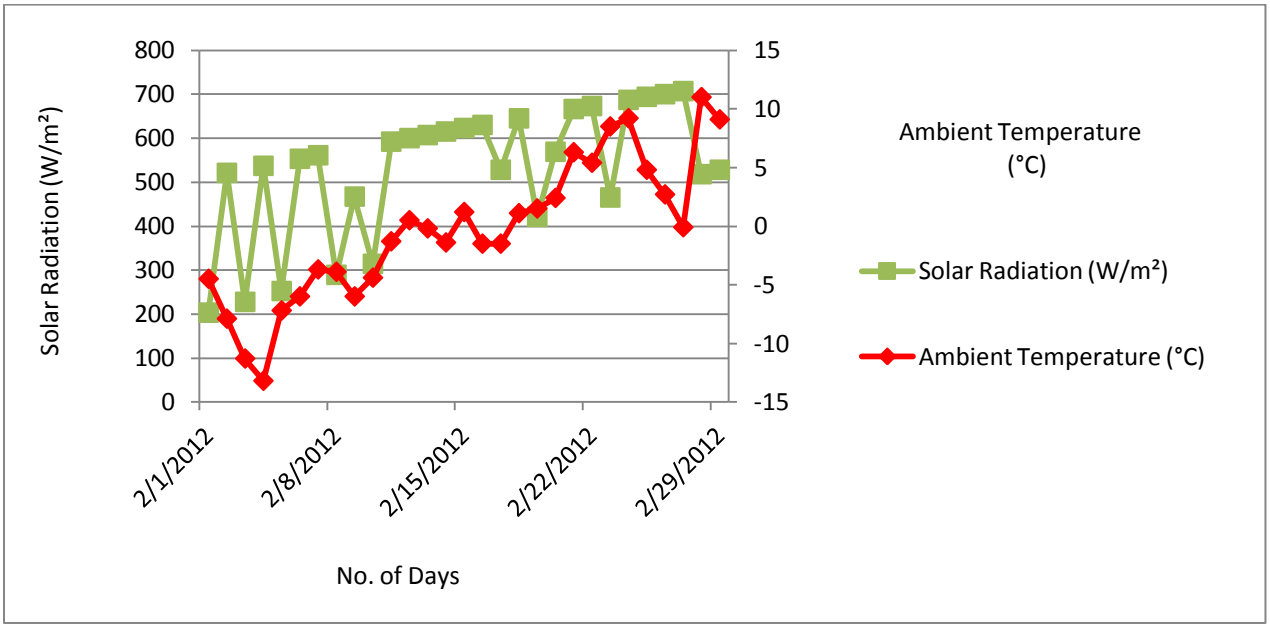

Figure A.2: Solar Radiation (W/m^2) versus Ambient Temperature (°C) in February

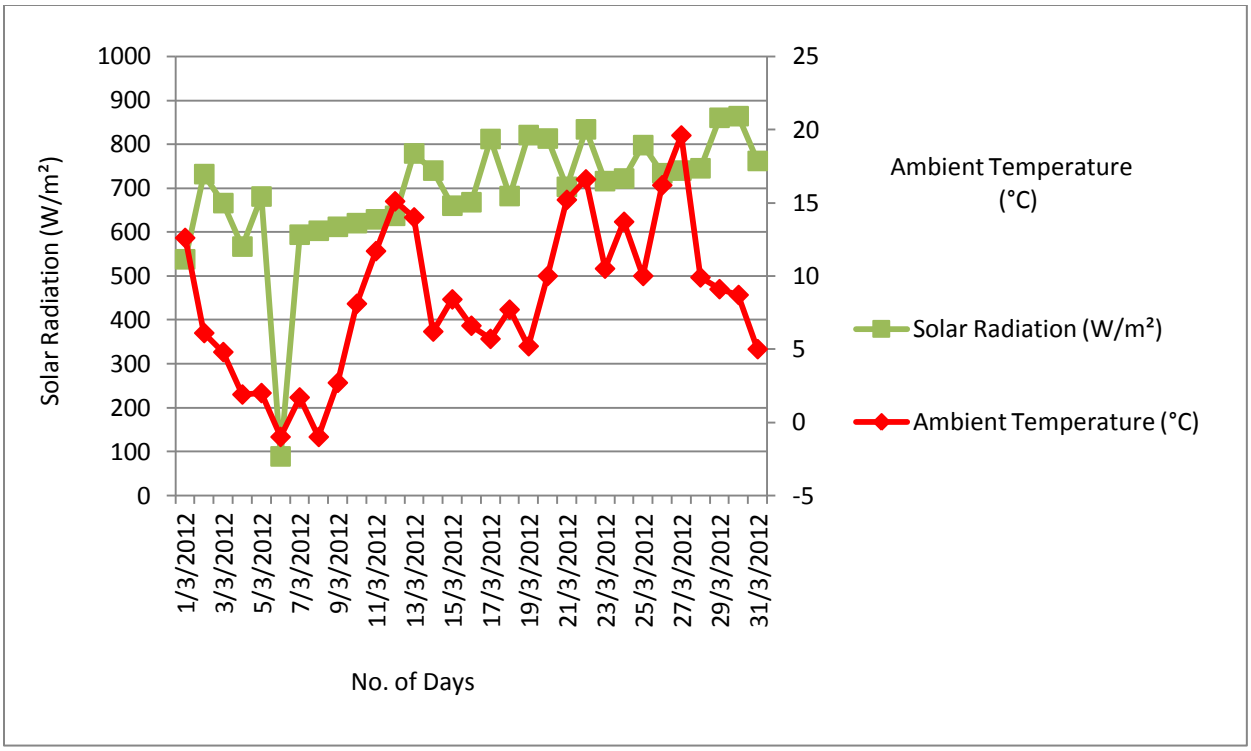

Figure A.3: Solar Radiation (W/m^2) versus Ambient Temperature (°C) in March

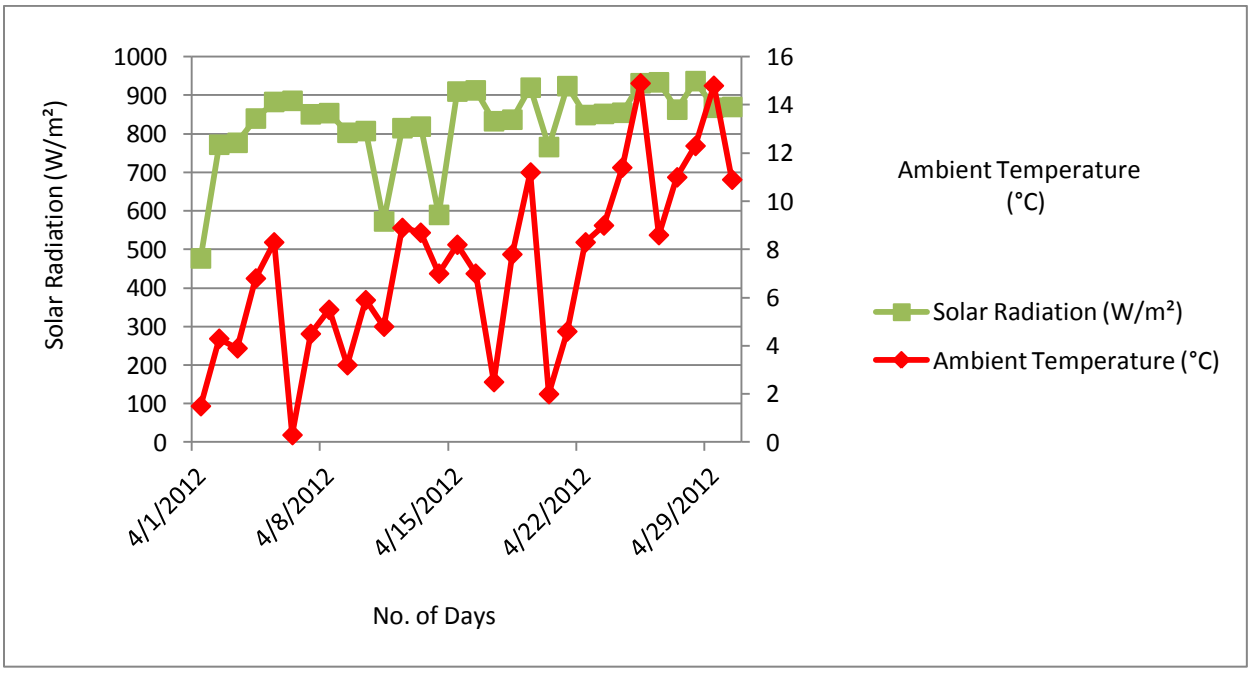

Figure A.4: Solar Radiation (W/m^2) versus Ambient Temperature (°C) in April

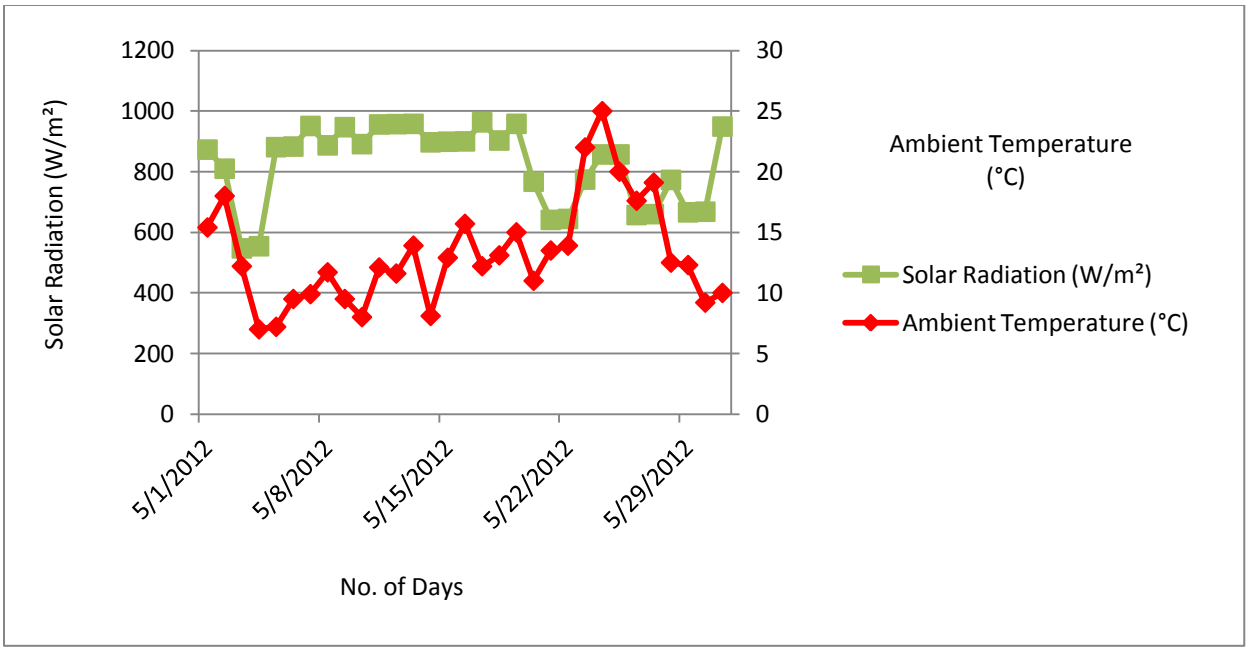

Figure A.5: Solar Radiation (W/m^2) versus Ambient Temperature (°C) in May

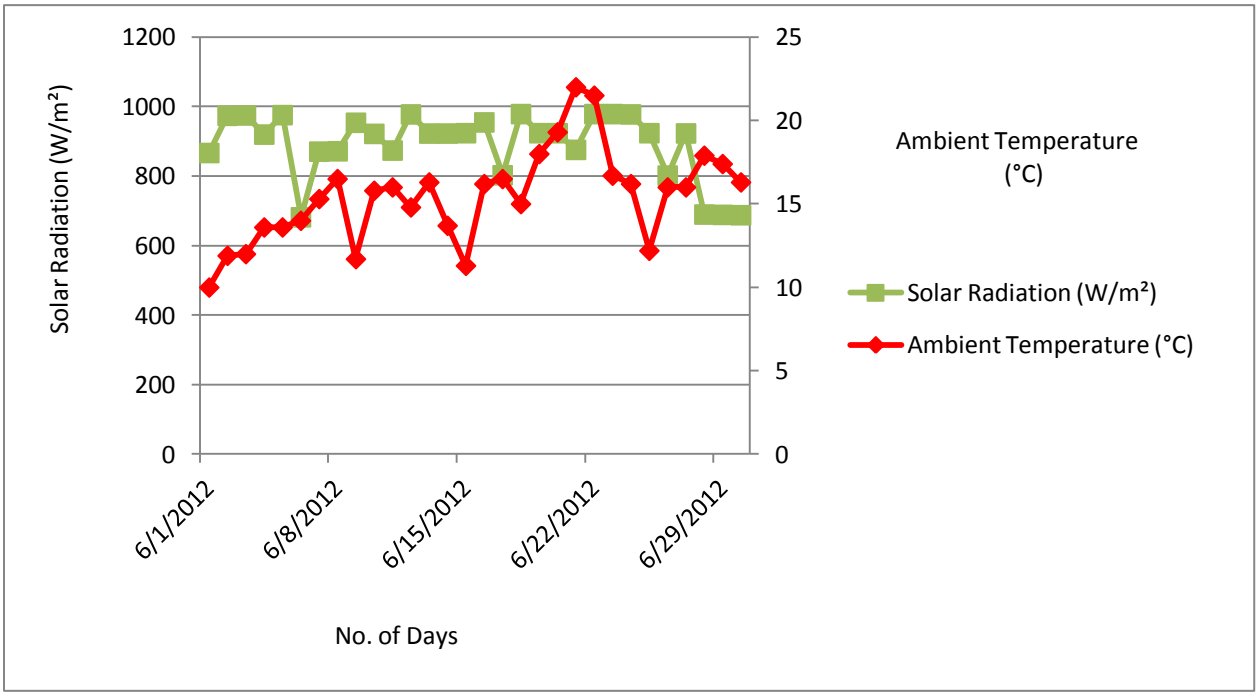

Figure A.6: Solar Radiation (W/m^2) versus Ambient Temperature (°C) in June

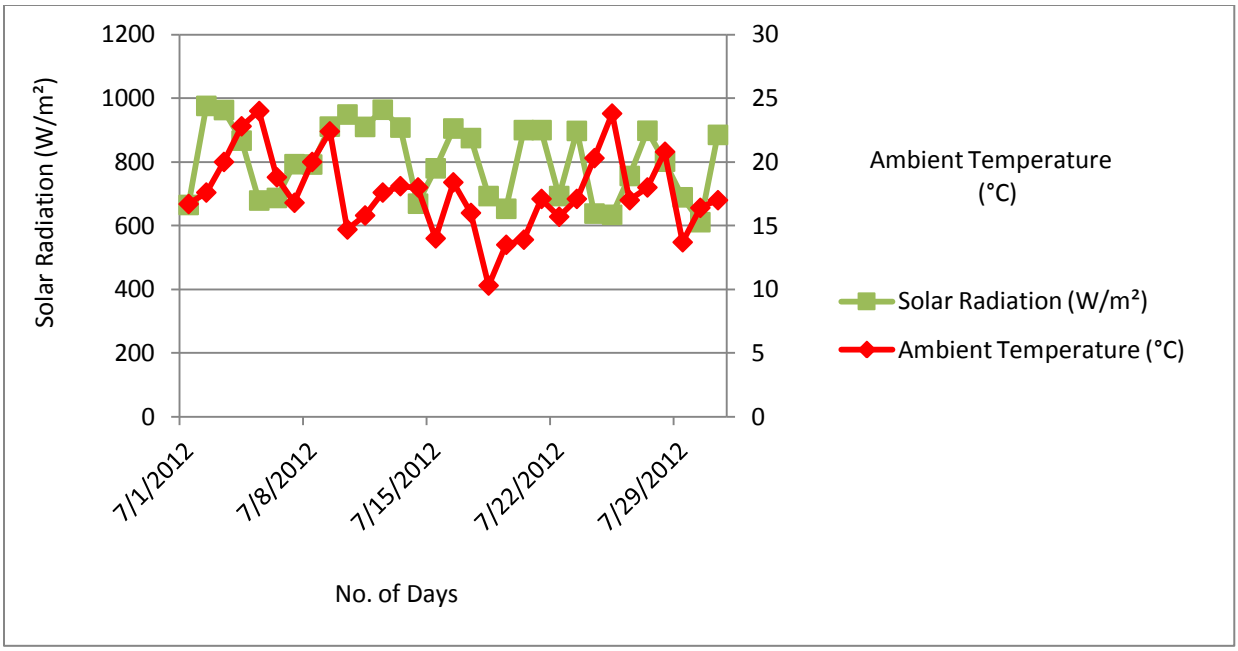

Figure A.7: Solar Radiation (W/m^2) versus Ambient Temperature (°C) in July

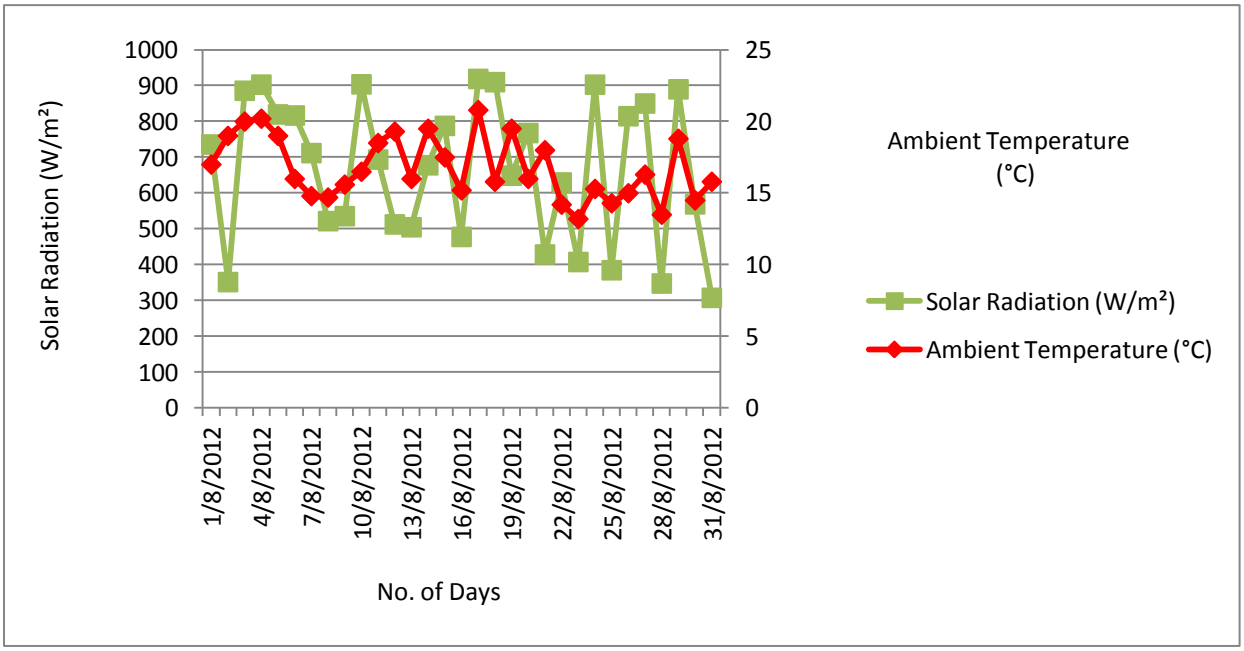

Figure A.8: Solar Radiation (W/m^2) versus Ambient Temperature (°C) in August

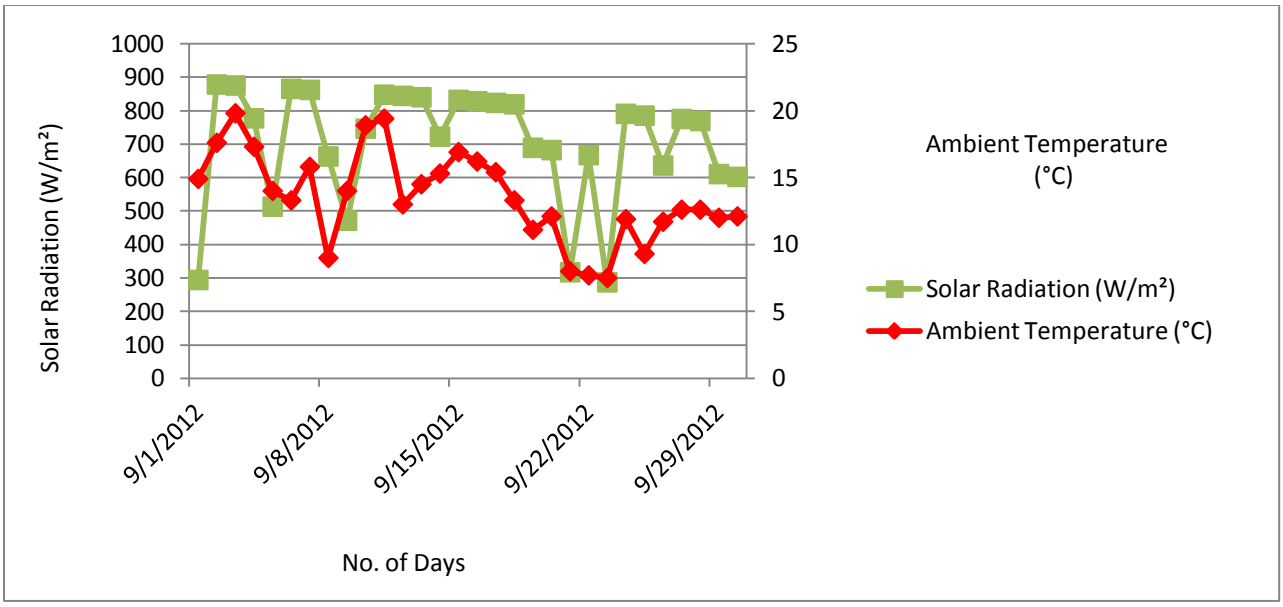

Figure A.9: Solar Radiation (W/m^2) versus Ambient Temperature (°C) in September

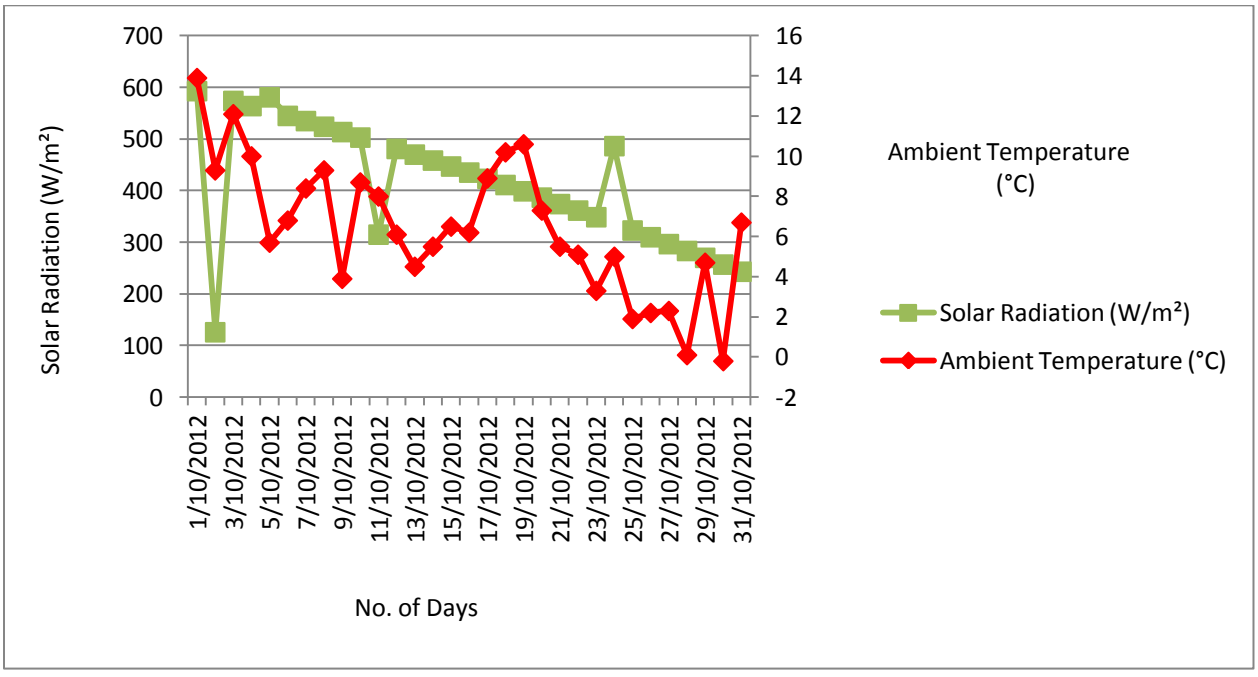

Figure A.10: Solar Radiation (W/m^2) versus Ambient Temperature (°C) in October

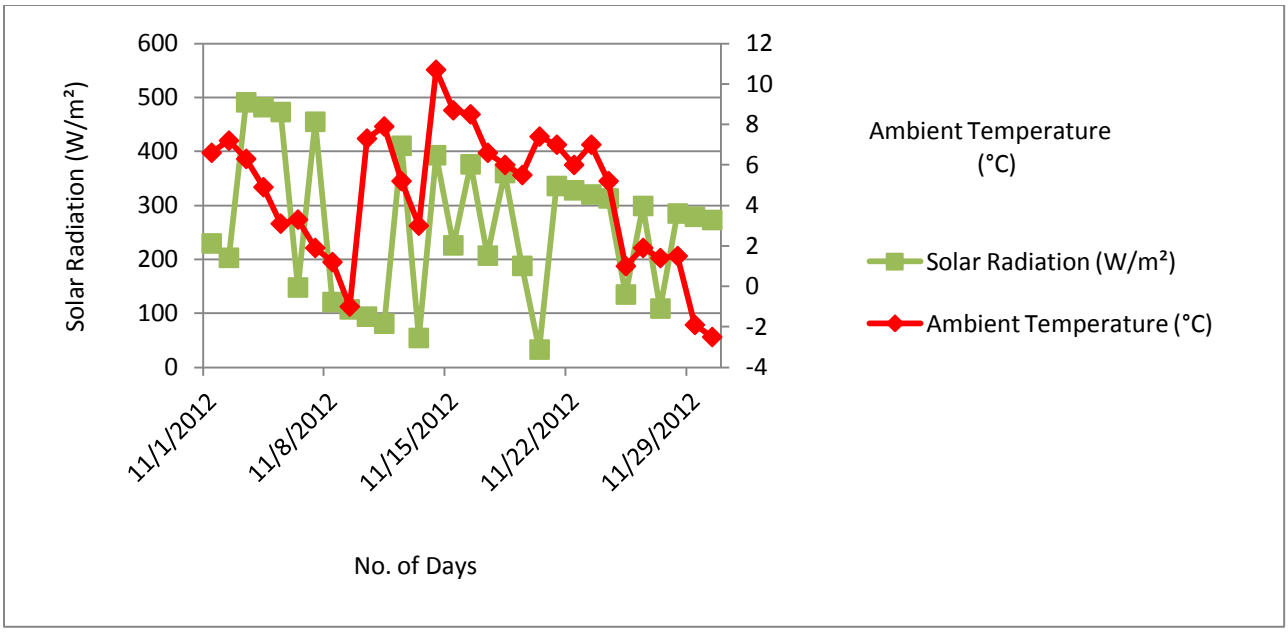

Figure A.11: Solar Radiation (W/m^2) versus Ambient Temperature (°C) in November

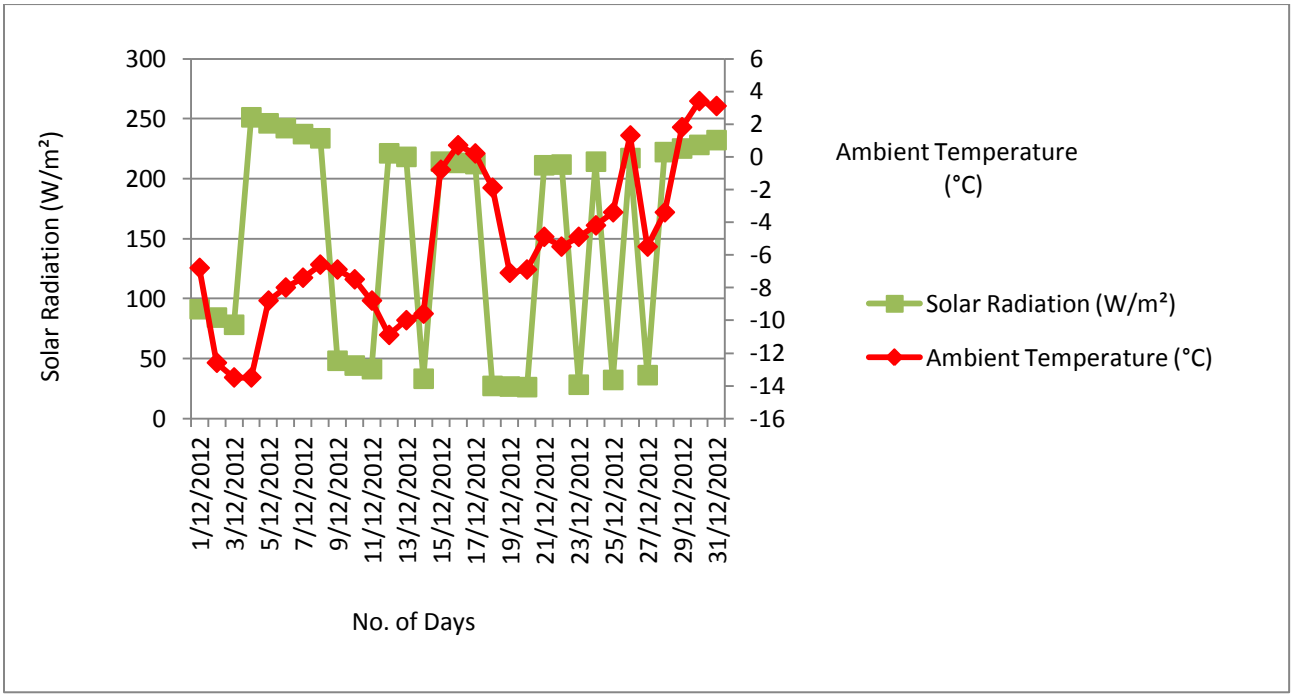

Figure A.12: Solar Radiation (W/m^2) versus Ambient Temperature (°C) in December

APPENDIX B

Line Current (A) versus Conductor Temperature (°C)

In this appendix, the current flowing through the overhead conductor (VL3) versus its temperature is shown in detail based on the calculations done for all the months of year 2012.

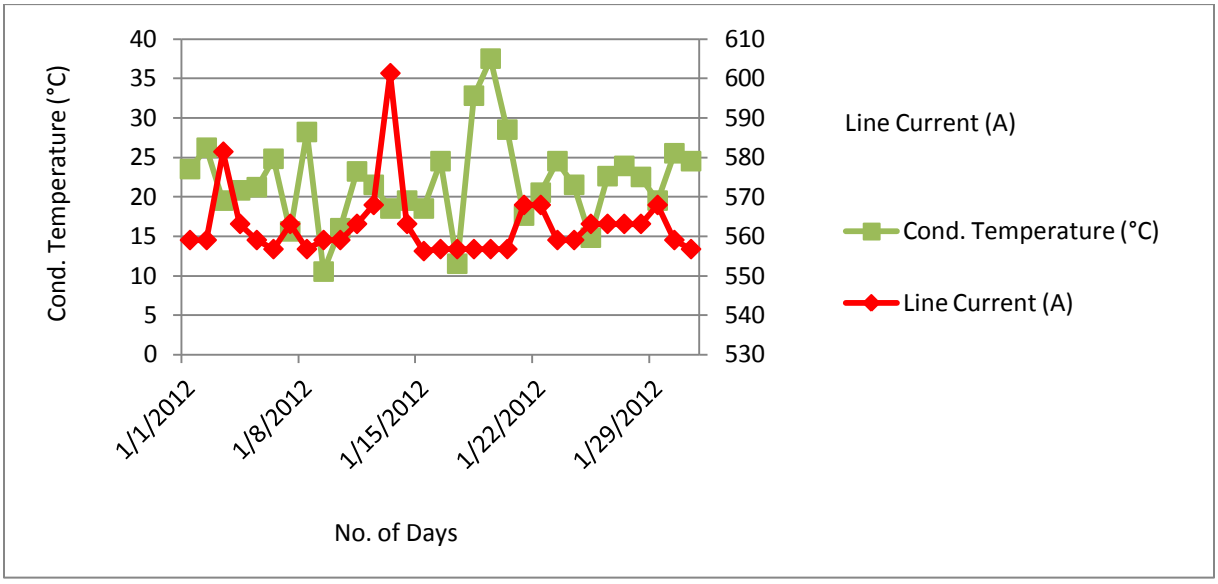

Figure B.1: Line Current (A) versus Conductor Temperature (°C) in January

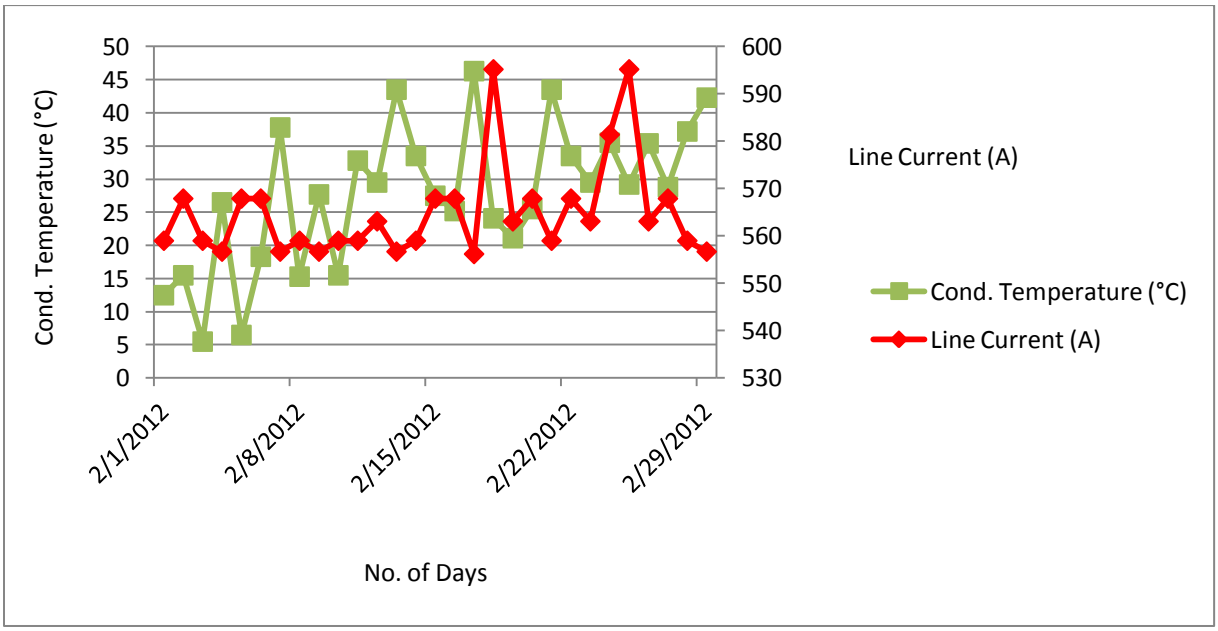

Figure B.2: Line Current (A) versus Conductor Temperature (°C) in February

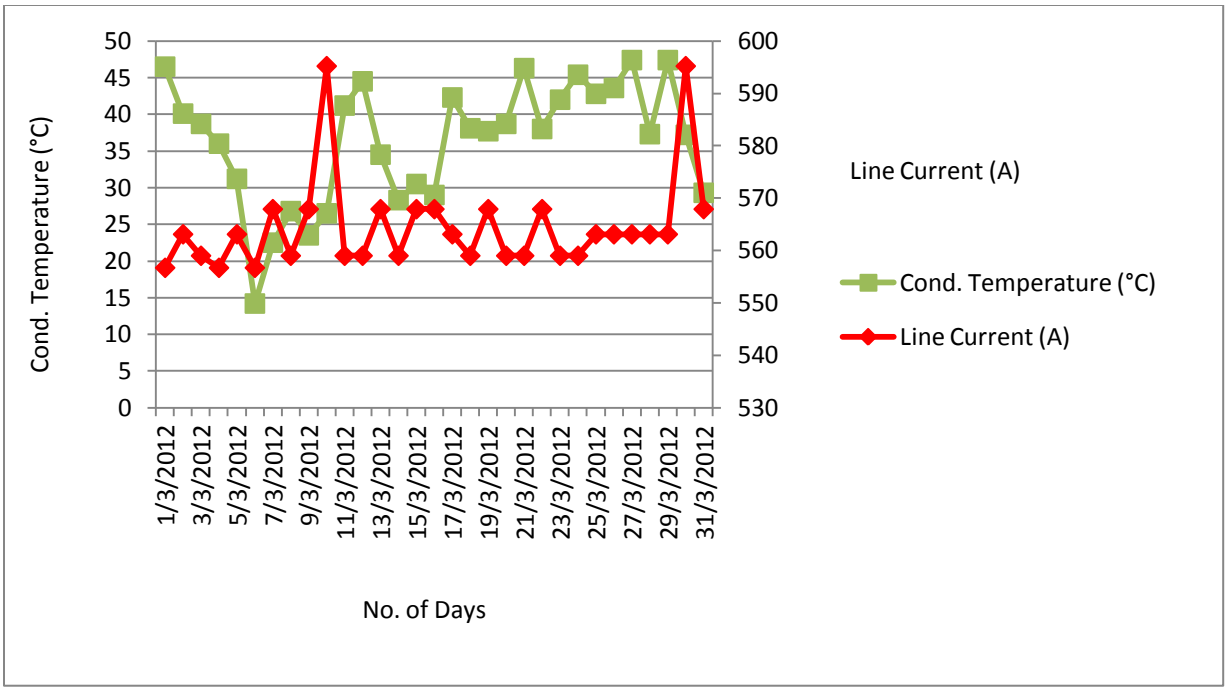

Figure B.3: Line Current (A) versus Conductor Temperature (°C) in March

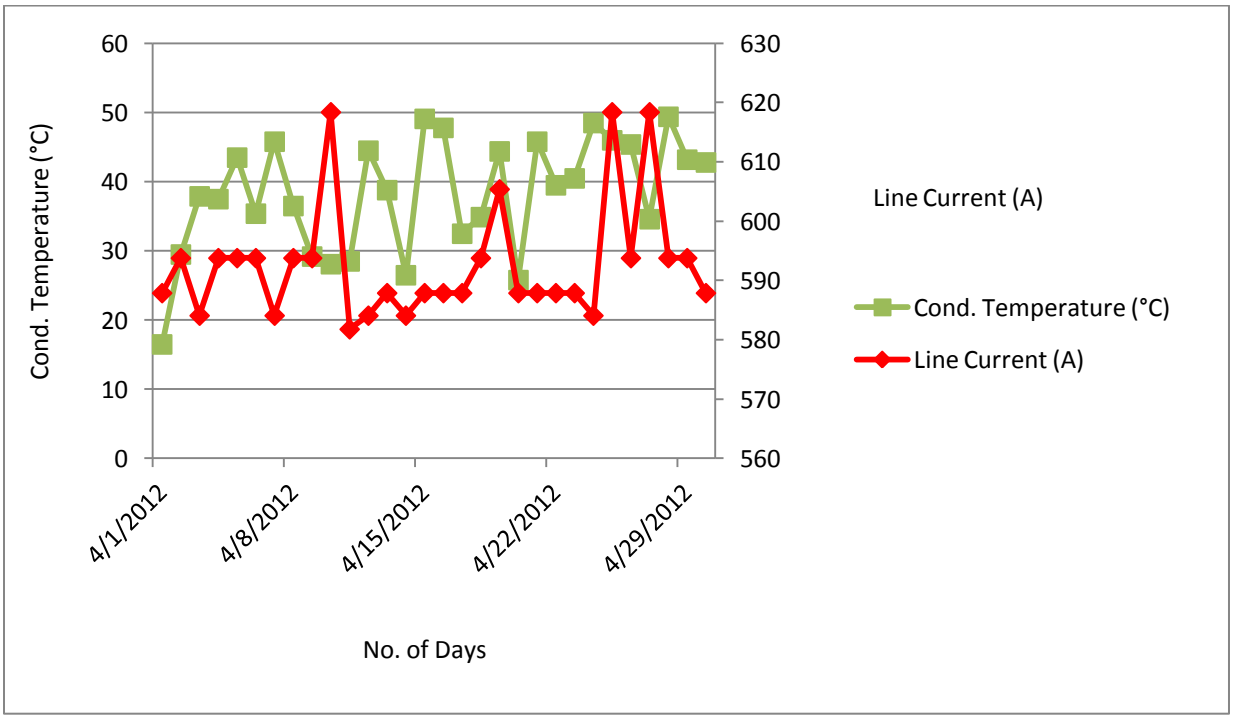

Figure B.4: Line Current (A) versus Conductor Temperature (°C) in April

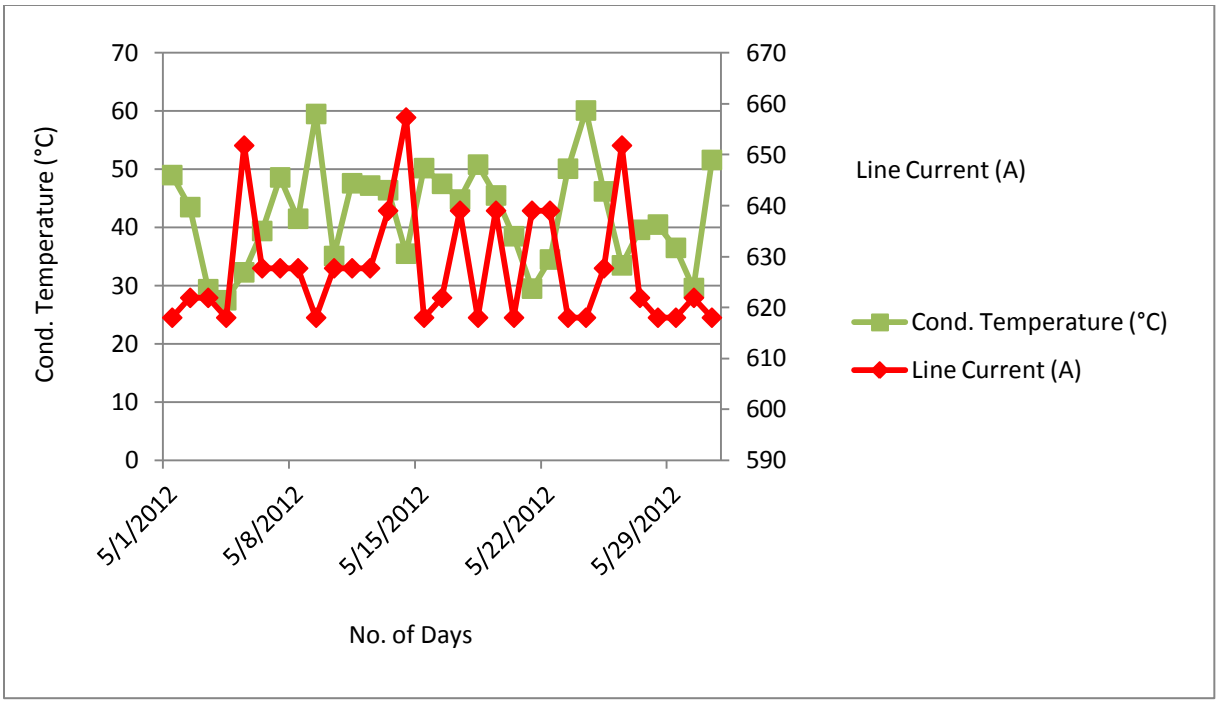

Figure B.5: Line Current (A) versus Conductor Temperature (°C) in May

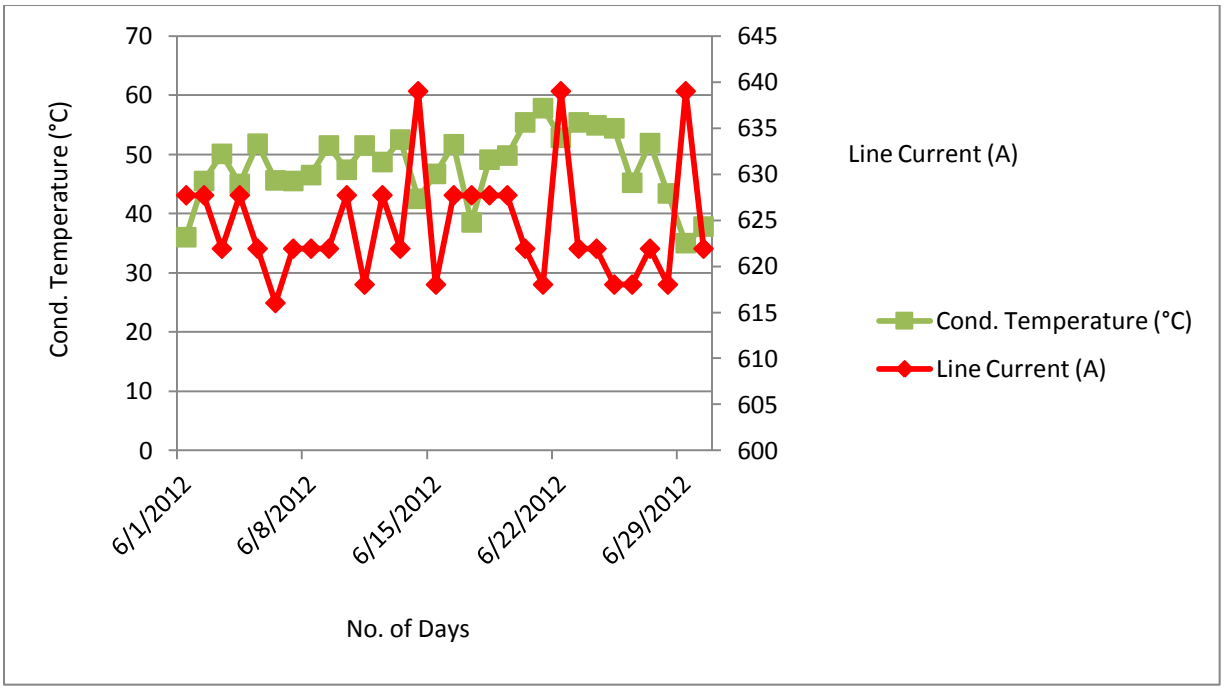

Figure B.6: Line Current (A) versus Conductor Temperature (°C) in June

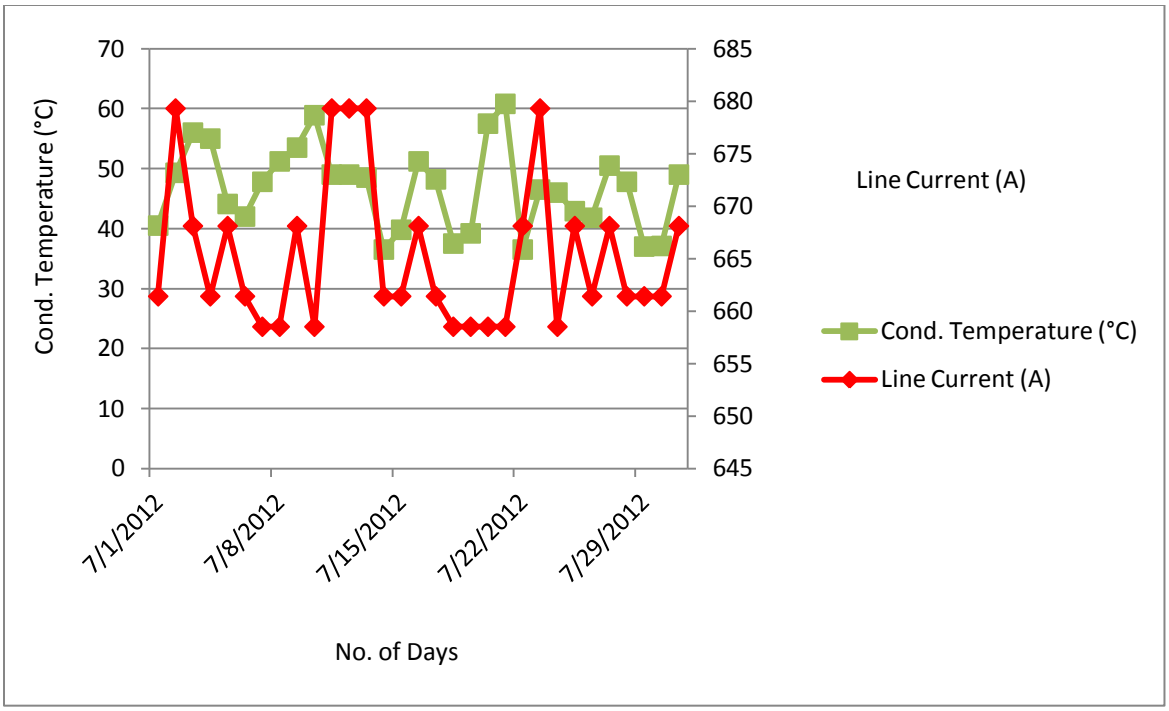

Figure B.7: Line Current (A) versus Conductor Temperature (°C) in July

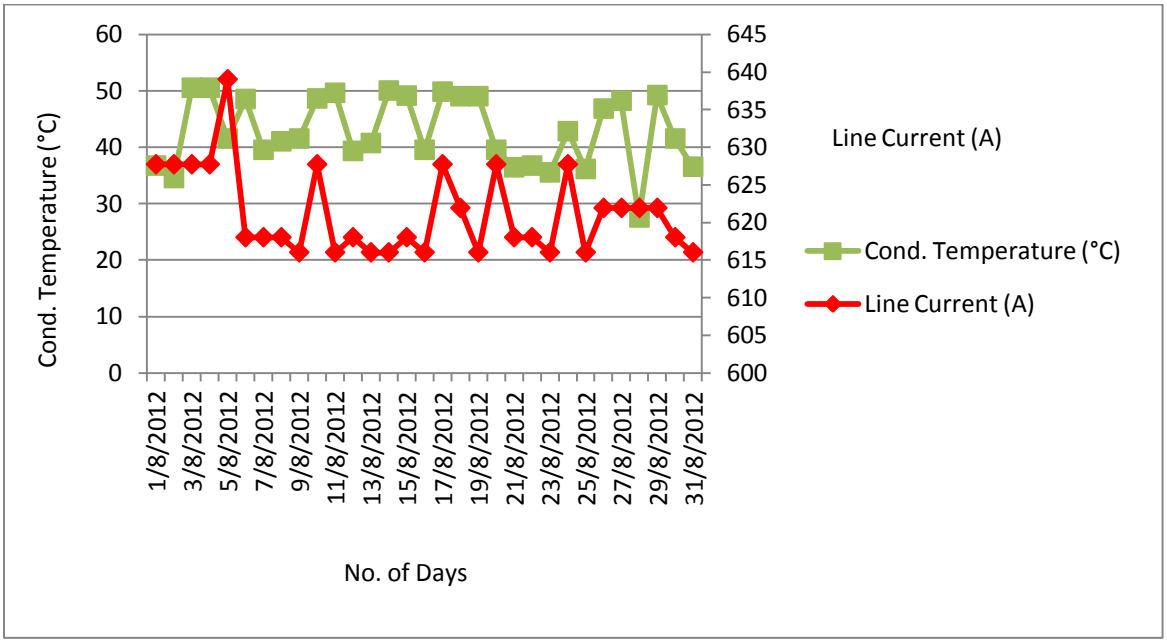

Figure B.8: Line Current (A) versus Conductor Temperature (°C) in August

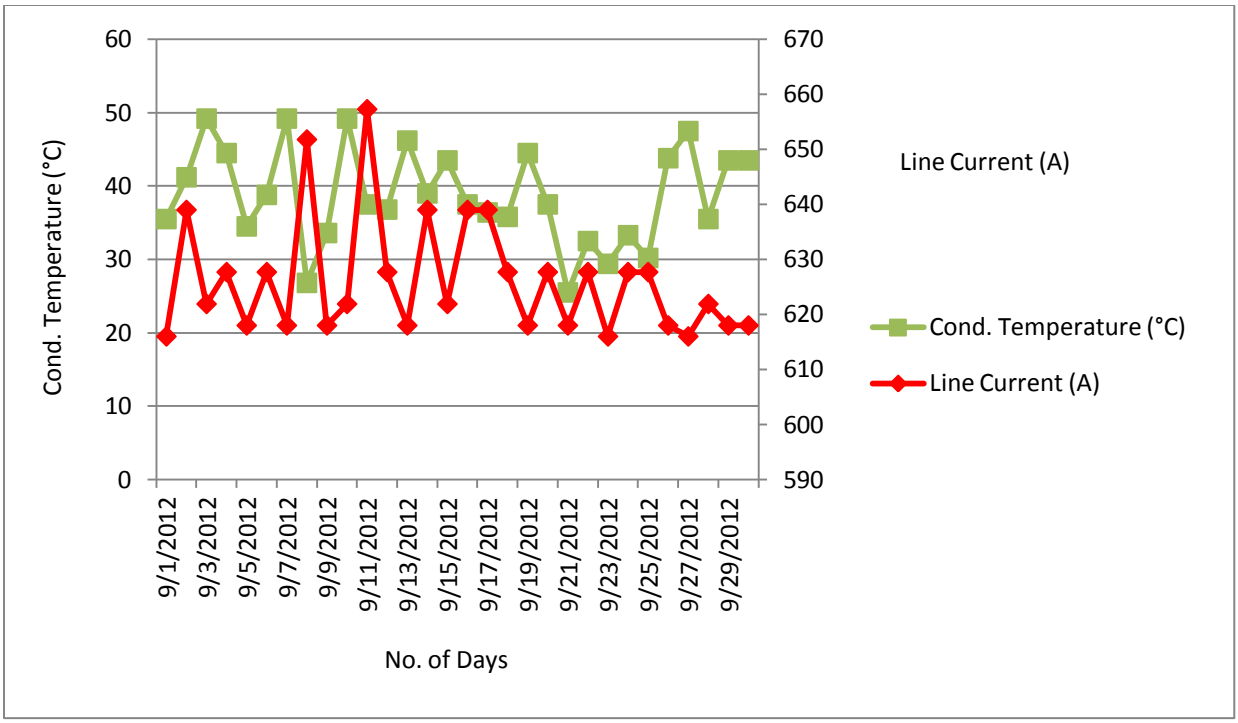

Figure B.9: Line Current (A) versus Conductor Temperature (°C) in September

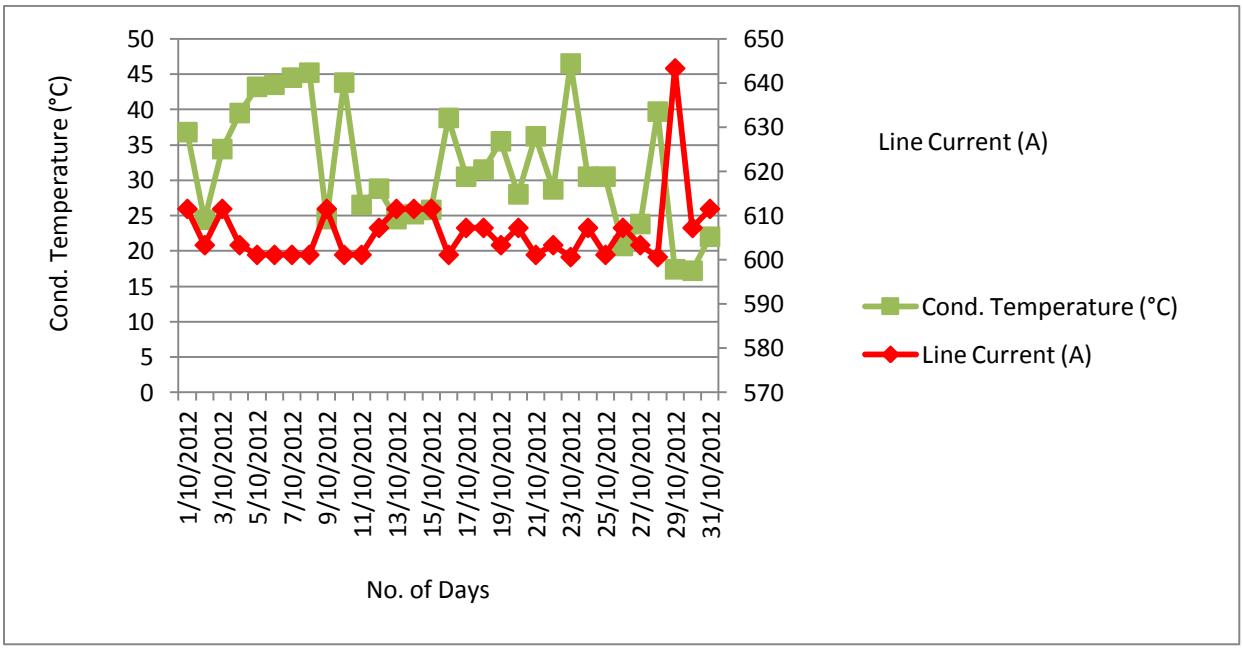

Figure B.10: Line Current (A) versus Conductor Temperature (°C) in October

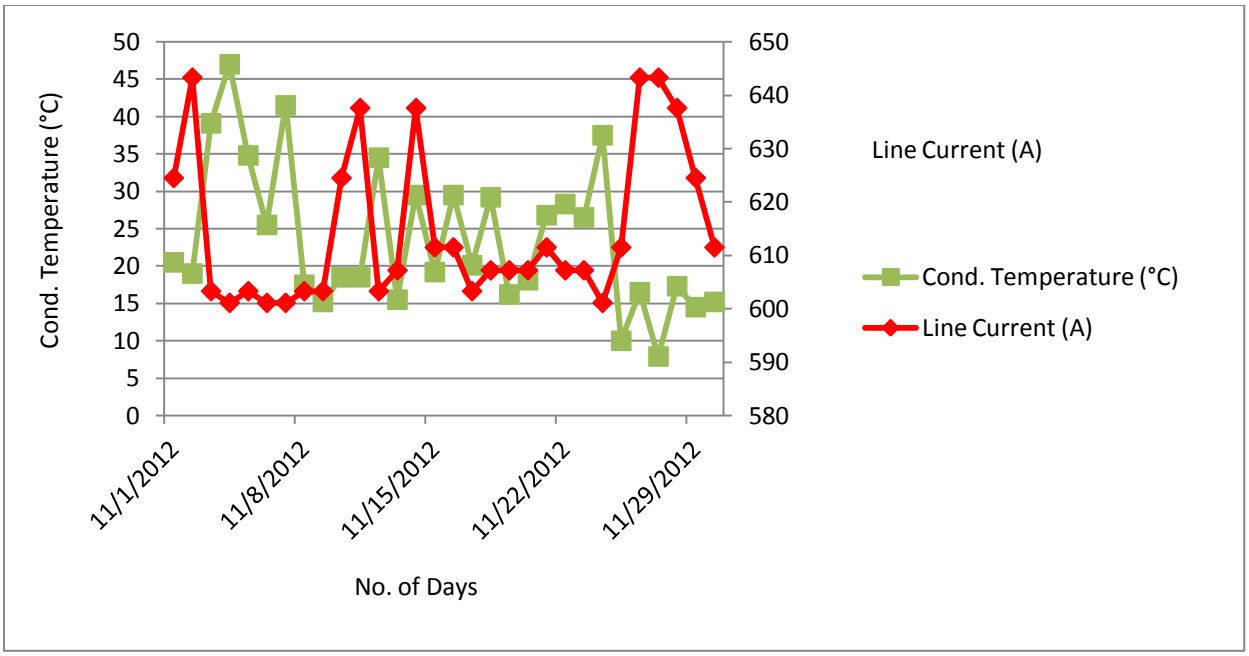

Figure B.11: Line Current (A) versus Conductor Temperature (°C) in November

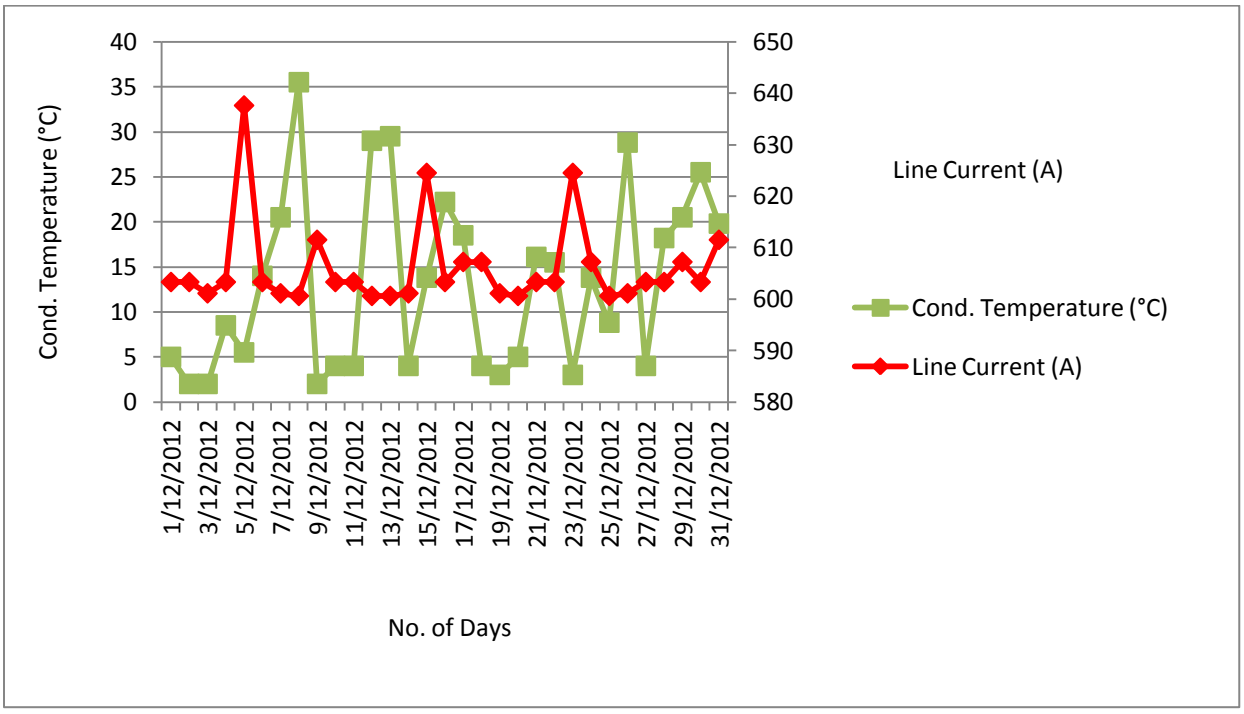

Figure B.12: Line Current (A) versus Conductor Temperature (°C) in December

APPENDIX C

The yearly based static and dynamic ampacities versus the line current

This appendix includes the static and dynamic ampacities for the VL3 overhead line as well as the actual current flowing through this conductor during each month of year 2012 with detailed analysis.

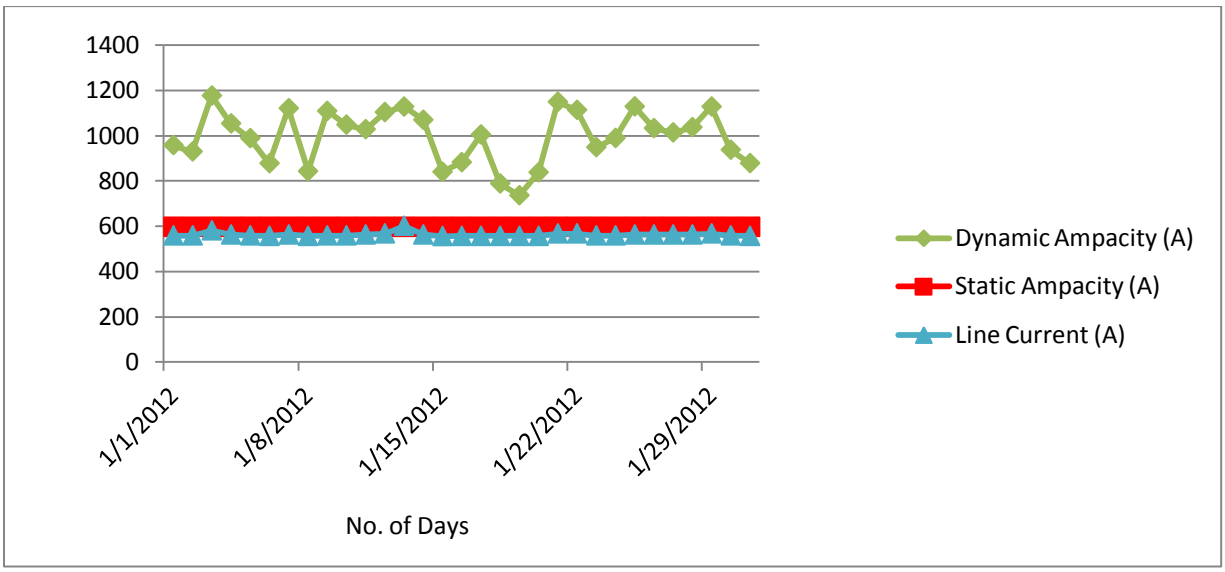

Figure C.1: Dynamic and Static Ampacities (A) with Line Current (A) in January

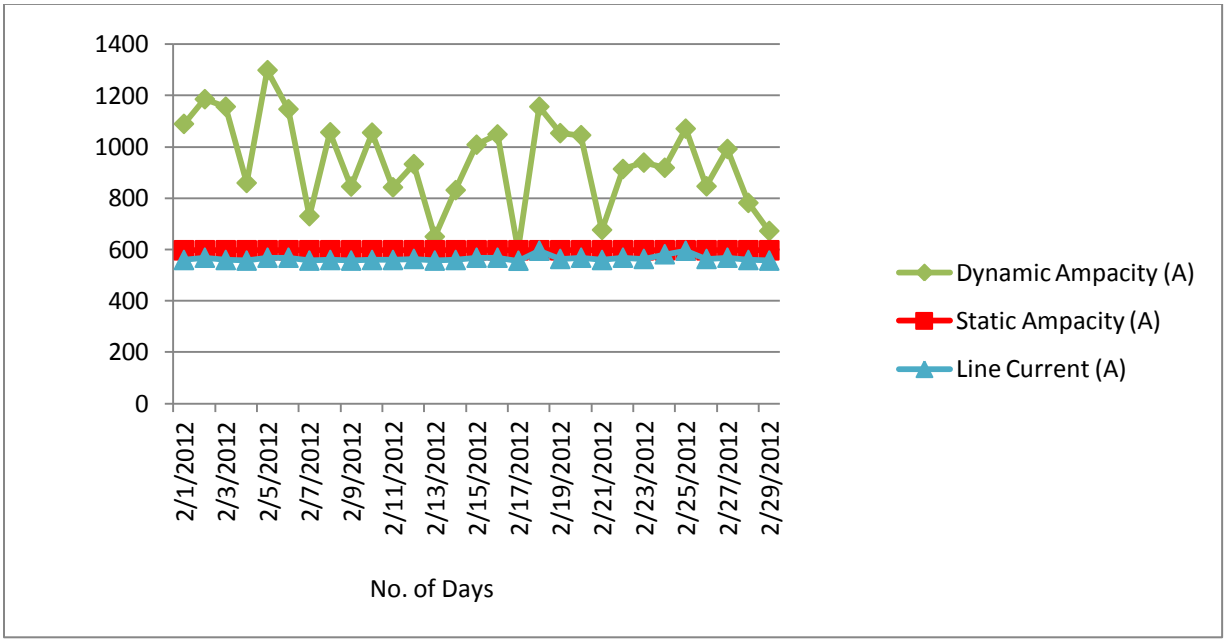

Figure C.2: Dynamic and Static Ampacities (A) with Line Current (A) in February

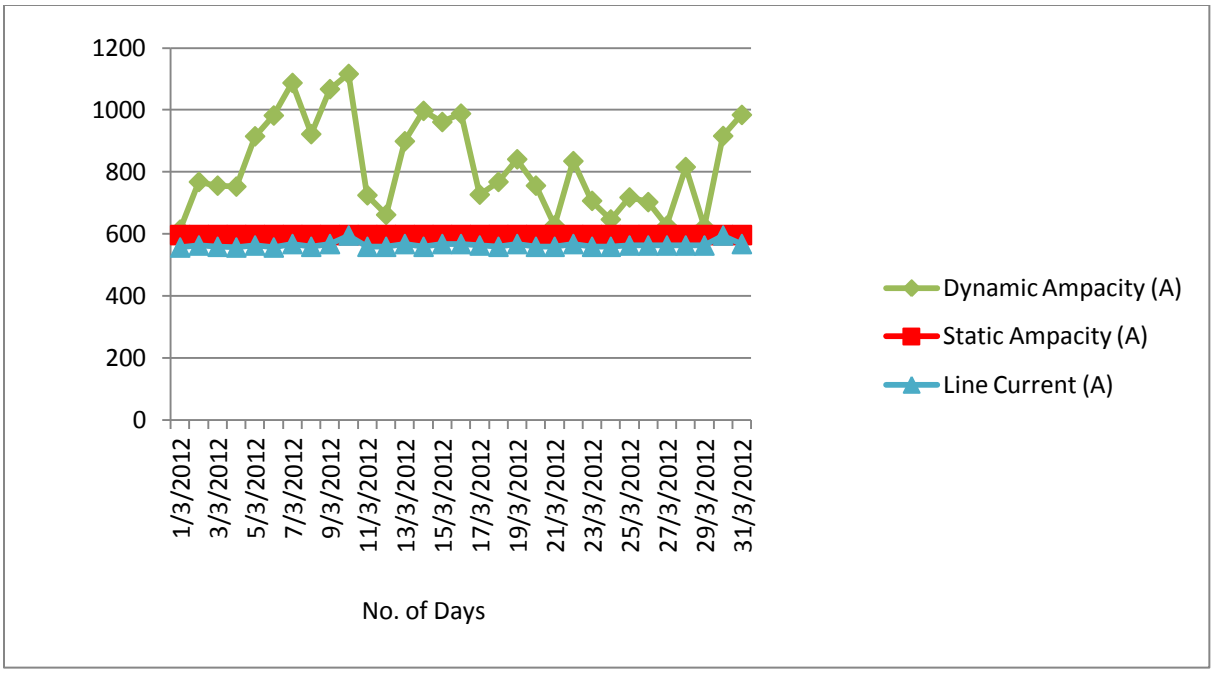

Figure C.3: Dynamic and Static Ampacities (A) with Line Current (A) in March

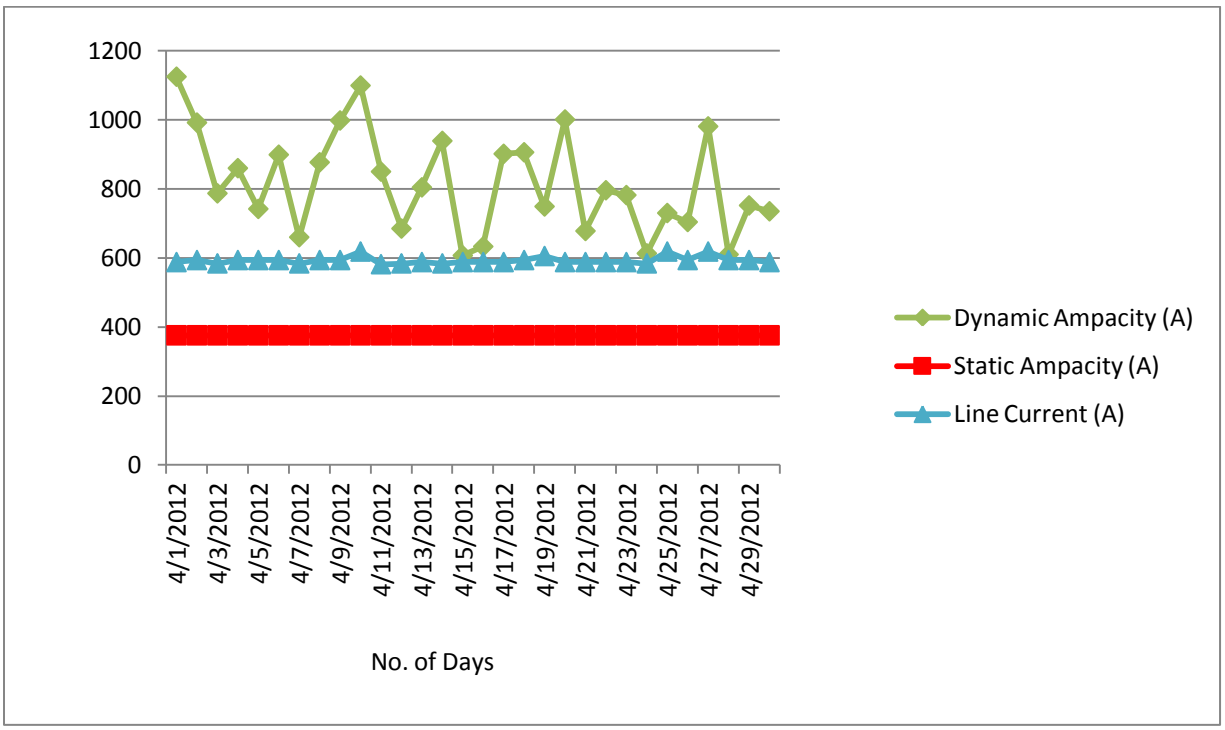

Figure C.4: Dynamic and Static Ampacities (A) with Line Current (A) in April

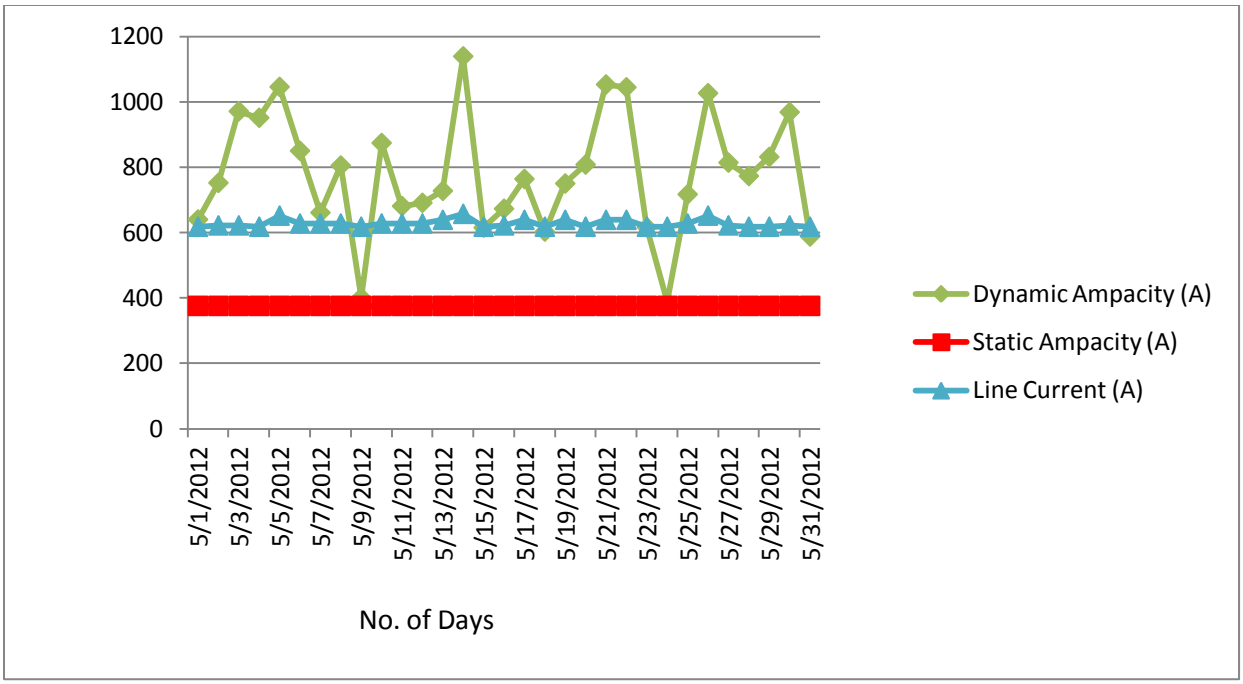

Figure C.5: Dynamic and Static Ampacities (A) with Line Current (A) in May

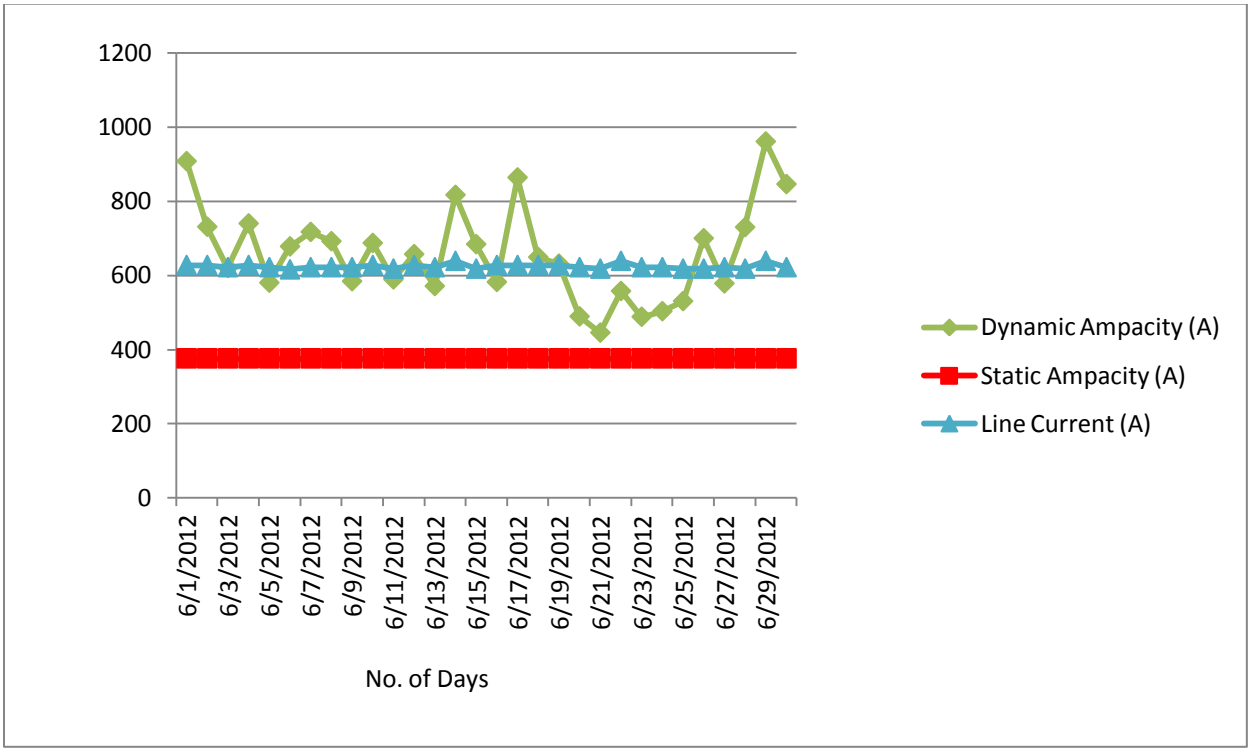

Figure C.6: Dynamic and Static Ampacities (A) with Line Current (A) in June

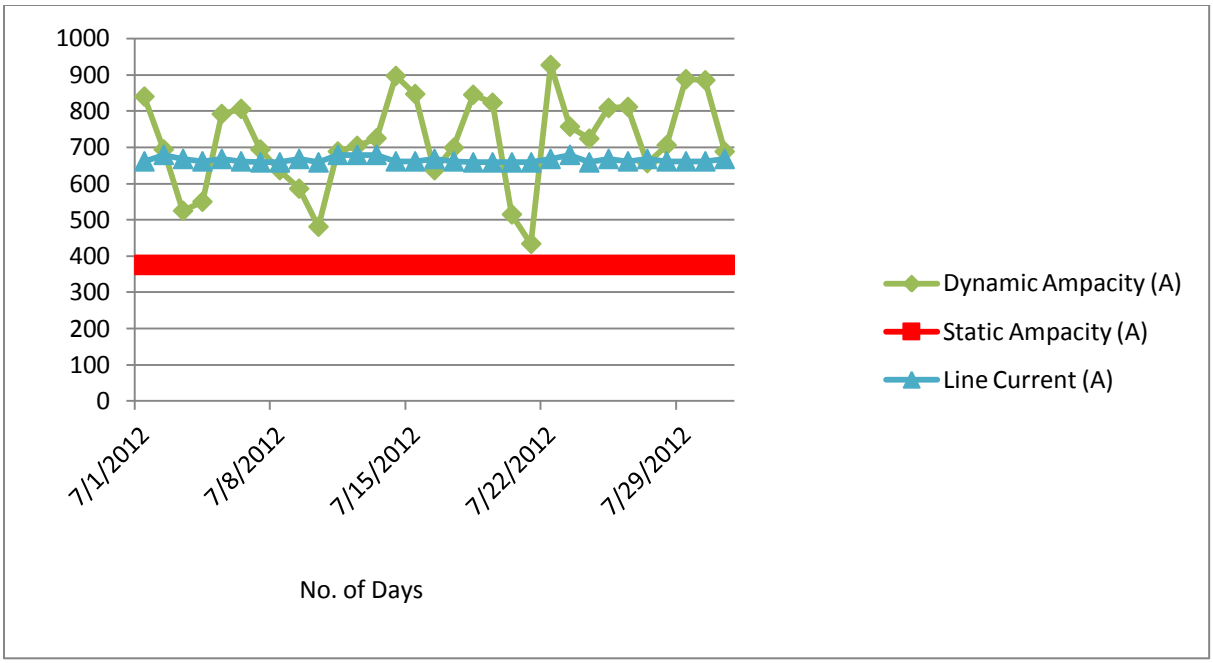

Figure C.7: Dynamic and Static Ampacities (A) with Line Current (A) in July

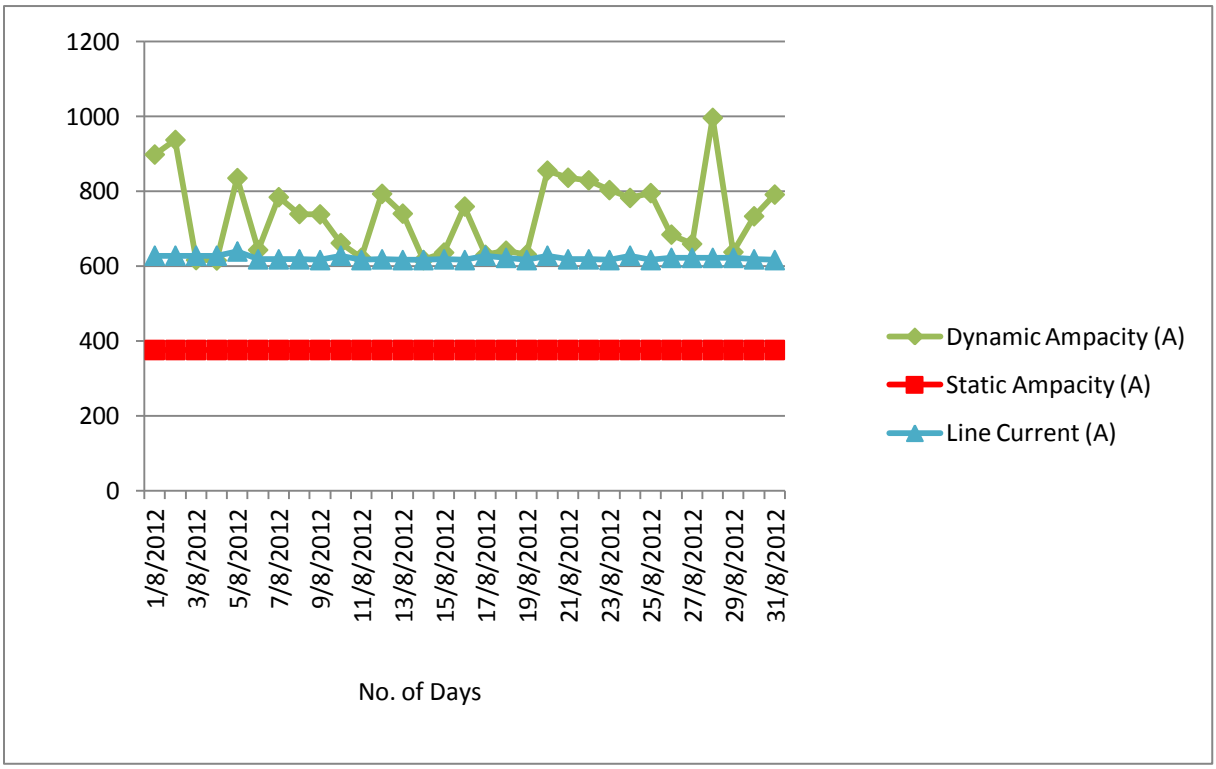

Figure C.8: Dynamic and Static Ampacities (A) with Line Current (A) in August

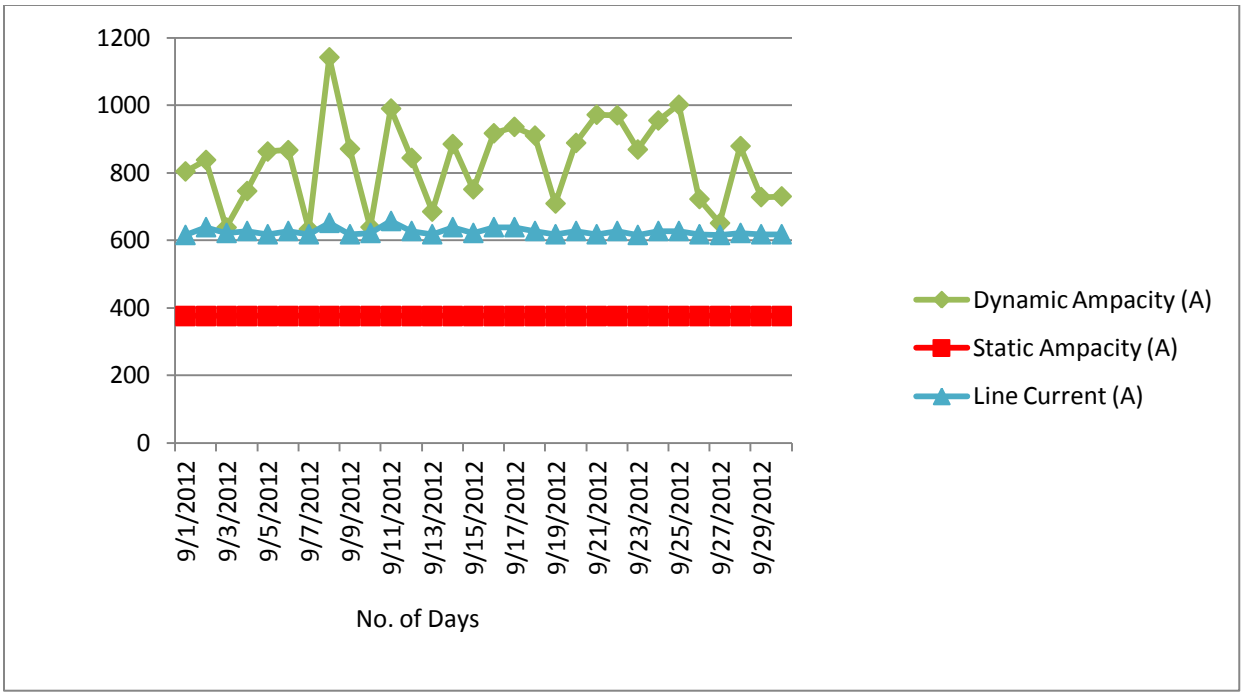

Figure C.9: Dynamic and Static Ampacities (A) with Line Current (A) in September

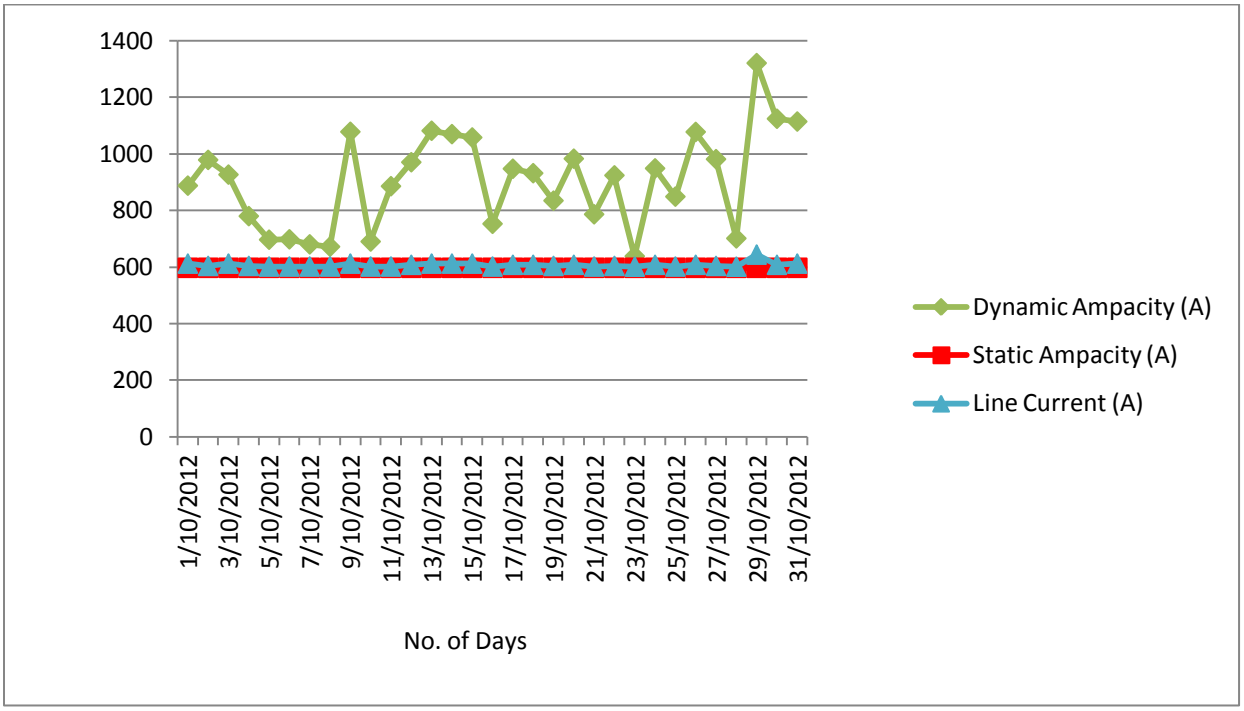

Figure C.10: Dynamic and Static Ampacities (A) with Line Current (A) in October

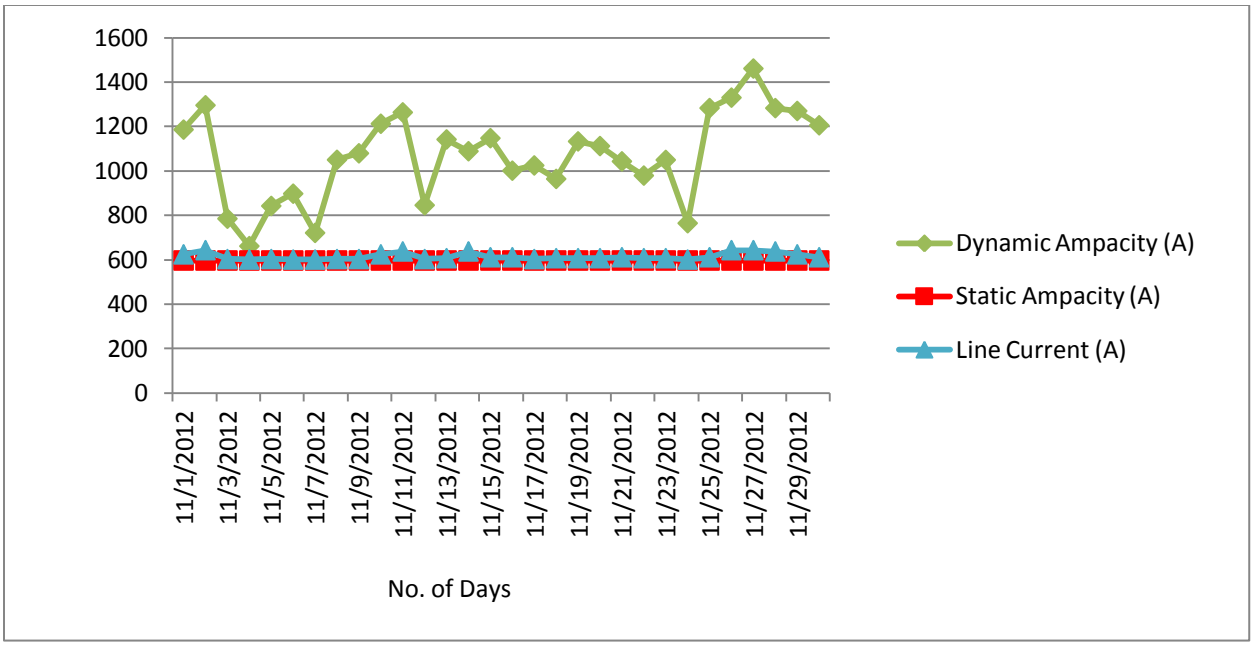

Figure C.11: Dynamic and Static Ampacities (A) with Line Current (A) in November

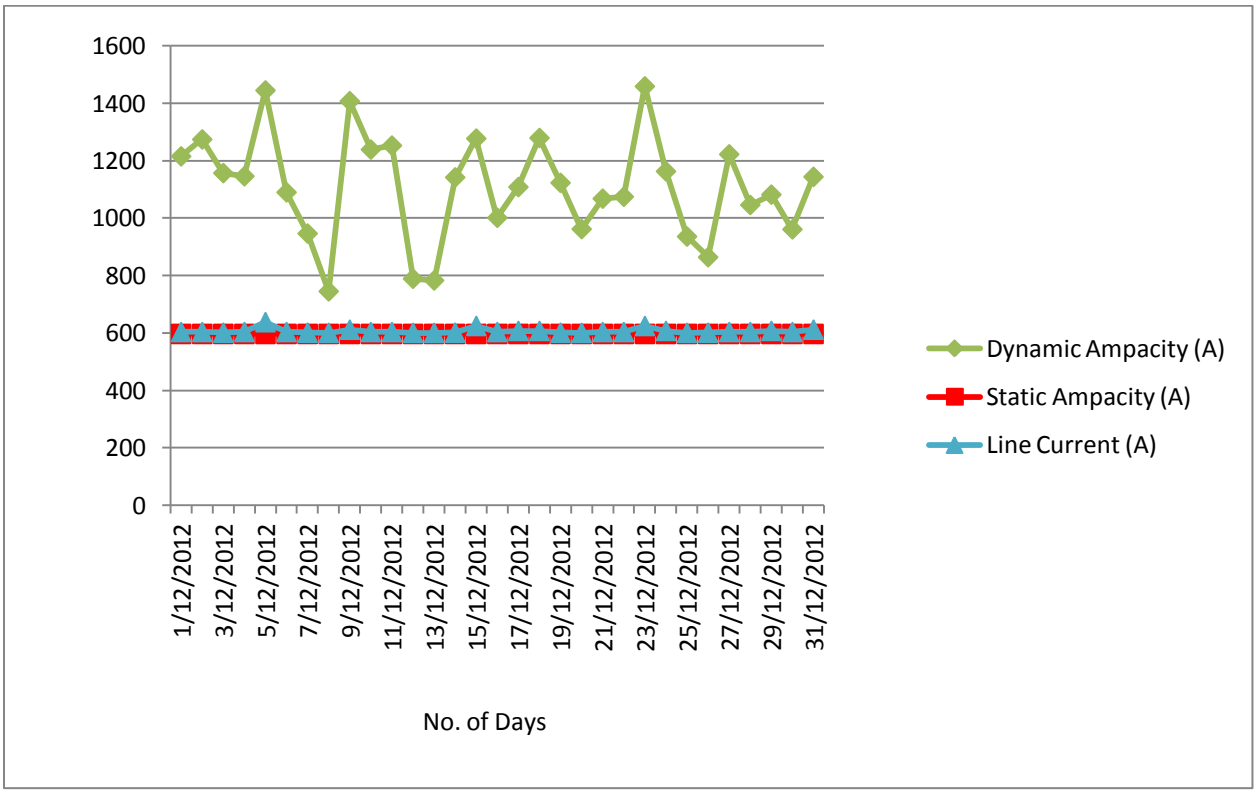

Figure C.12: Dynamic and Static Ampacities (A) with Line Current (A) in December